STRUCTURAL AND THREE-DIMENSIONAL INTERPRETATION OF AEROMAGNETIC ANOMALIES OVER PART OF THE IGNEOUS INTRUSIONS OF KANO STATE, NORTH-CENTRAL NIGERIA

BY

SULEIMAN, **MUHAMMED** ANKA
B.SC. (HONS) PHYSICS U.D.U,SOKOTO

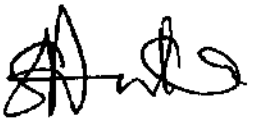
A THESIS SUBMITTED TO THE POST-GRADUATE SCHOOL AHMADU BELLO UNIVERSITY, ZARIA, IN PARTIAL FULFILMENT OF THE REQUIREMENTS FOR THE AWARD OF MASTER OF SCIENCE DEGREE IN APPLIED GEOPHYSICS.

DEPARTMENT OF PHYSICS
FACULTY OF SCIENCE
AHMADU BELLO UNIVERSITY
ZARIA, NIGERIA

JULY 1998

DECLARATION

The report presented in this thesis is not a published, or unpublished work of others, it is the result of an original study carried out by this author. To the best of my knowledge, it has not been submitted in whatever form to any other institution, organization or body other than the Ahmadu Bello University for the award of a degree. Where the work of others are made use of, such sources are appropriately acknowledged and referenced.



CERTIFICATION

This thesis entitled "Structural and Three-Dimensional Interpretation of Aeromagnetic Anomalies over part of the Igneous Intrusions of Kano State, North-Central Nigeria." by Suleiman, Muhammed Anka meets the regulations governing the Award of the degree of Master of Science of Ahmadu Bello University and is approved for its contribution to knowledge and literary presentation.

Prof. S.B. Ojo
Chairman, Supervisory Committee.

Date: 03/11/98

Prof. I.B. Osazuwa
Member, Supervisory Committee.

Date: 05/11/98

Prof. I.B. Osazuwa
Head of Physics Department.

Date: 05/11/98

Prof. J.Y. Olayemi
Dean, Postgraduate School.

Date: 13/4/99

DEDICATION

Dedicated to my mother, Mrs Hadizatu Suleiman Anka.
For being a loving and caring mother

ACKNOWLEDGEMENTS

All praise be to Allah for granting me the opportunity to undertake this work. My sincere gratitude and heartfelt indebtedness to my Supervisor Prof. S.B. Ojo for initiating the topic of the research. His invaluable guidance, keen interest and advice which he readily gave at all times during the work and in writing this report is keenly appreciated. I am equally grateful to my other supervisor Prof. I.B. Osazuwa, Head of Department of Physics, for his guidance and advice; he willingly made available to me his invaluable research materials and computing facilities and personally supervised the completion of this work. This gesture is well appreciated. I am also grateful to Dr. Roland Kangkolo for making available his computer programs to me; his advice and suggestions in the use of the computer is well appreciated.

Also, I wish to say thanks to all the staff members of the Geophysics Unit for their help during the course work and in the period of my stay in the department. Thanks to my course mates Akaolisa C. Zanders, Mohammed Salisu, Mohammed Saleh, and Mohammed Adamu to mention, but a few. I have to metion the help rendered by my family, my brothers Alh. Sani Suleiman Anka, Alh. Sani Salihu Anka and Ibrahim Suleiman Anka for their brotherly advice, encouragement and financial assistance. May Allah reward them abundantly. Amin. The facilities provided by the International Programme in the Physical Sciences, Uppsala University, Sweden for research work in the department, also made it possible to complete the work on schedule, this is highly acknowledged.

ABSTRACT

An interpretation of aeromagnetic data has been carried out over an area of the Precambrian to early Palaeozoic basement rocks of Kano State, North-central Nigeria, between Latitudes 11°00'N to I2°00'N and Longitudes 8°00'E and 9°00'E. The interpretation covers the areas of igneous intrusions of the basement.

Non-orientational and orientational studies of the lineament features reveal NE-SW and E-W trends characterizing the area. Statistical analysis using the analytical method of auto-covariance confirms this result. The residual and second derivative maps emphasize the shallow features of the area. These features correlate very well with the previous gravity investigation within the area. The regional field and upward continuation map reflect deep seated structures in the area and shows the regional structures field have an E-W trend. This studies show that the area is characterized by NE-SW residuals superimposed on an E-W treading regional field. Residual anomalies of both high and low amplitude are recognized on the residual map which are oriented along the interpreted shear zone.

A 3-Dimension interpretational method has been used for the inversion of these anomalies. A preliminary spectral analysis reveals a shallow depth magnetic horizon of 0.45 to 0.65 km and a deeper layer with depth of 5.2 km to 6.8 km for the rock ensembles. The results obtained from the inversion method show that the depth to the tops of the modelled bodies vary from zero to 1.47 km and the depth to the bottom varying from 0.601 km to 8.628 km. With variation in the susceptibility contrast from -0.00120 emu. to +0.0833 emu. The positive susceptibilities are interpreted to be due to basic igneous intrusions, while the negative susceptibilities are due to acidic intrusions.

I

TABLE OF CONTENTS

Page

TITLE PAGE i

DECLARATION ii

CERTIFICATION iii

DEDICATION iv

ACKNOWLEDGEMENT v

ABSTRACT vi

TABLE OF CONTENTS xi

LIST OF FIGURES xiii

LIST OF TABLES ix

CHAPTER ONE

1.0 INTRODUCTION 1

1.1 The Study Area 2

1.2 Accessibility and Geography of the Study Area 4

1.3 Previous Geophysical Work Done 4

1.4 Aim and Objectives of the Study 6

1.5 Scope of the Study 7

CHAPTER TWO

2.1 GENERAL GEOLOGY 8

2.1.0 Introduction 8

2.1.1 The Migmatite Gneiss-Quartzite Complex 10

2.1.2 The Older Granites 11

2.2 LOCAL GEOLOGY 11

2.3 Rock Types 13

2.3.1 Migmatites 13

2.3.2 Gneisses 13

2.3.3 Granites 15

2.3.4 Basic Intrusives 15

2.3.5 Superficial Deposits 15

2.4 STRUCTURES 16

2.4.1 Fractures 16

CHAPTER THREE

3.0 THEORY OF MAGNETIC METHOD 17

3.1 DEFINITIONS.....17

3.1.1 Magnetic poles 17

3.1.2 Magnetic force 17

3.1.3 Magnetic Field 18

3.1.4 Magnetic moment 18

3.1.5 Intensity of magnetization 18

3.1.6 Susceptibility 18

3.1.7 Permeability 20

3.1.8 Units of magnetic intensity 20

3.1.9 The geomagnetic field 21

3.1.10 Rock magnetization 21

3.2 Instruments used for magnetic measurement 22

3.3 Survey systems 23

3.4 Aeromagnetic survey 23

3.5 Reduction of aeromagnetic data 25

CHAPTER FOUR

4.0 DATA ACQUISITION, ANALYSIS AND INTERPRETATION 27

4.1 Data acquisition 27

4.1.1 Data setting 27

4.2 ANALYSIS AND INTERPRETATION 30

4.2.1 Introduction 30

4.3 Qualitative Interpretation 33

4.3.1 Correlation Between the Total Field Map and Geological Map 33

4.4 STRUCTURAL ANALYSIS 34

4.4.1 The Statistical Analysis of the Lineaments 34

4.5 Analytical Interpretation 38

4.5.1 Introduction 38

4.5.2 Separation of Residual and Regional Anomaly 38

4.5.3 Upward Continuation of the Total Field 39

4.5.4 The Auto Correlation Analysis 49

4.5.5 Second Vertical Derivative 51

4.6 General discussion on the structural trends 57

4.7 THREE DIMENSIONAL MODELLING

4.7.1 Introduction 59

4.7.2 Anomaly equations 63

4.7.3 Inversion 65

4.7.4 Approximate equations 68

4.8 Present application 70

4.8.1 Initial Parameters 70

4.8.2 Anomaly Number ANO 01 72

4.8.3 Anomaly Number ANO 02 75

4.8.4 Anomaly Number ANO 03 75

4.8.5 Anomaly Number ANO 04 77

4.8.6 Anomaly Number ANO 05 79

4.8.7 Anomaly Number ANO 06 83

4.8.8 Anomaly Number ANO 07 85

CHAPTER FIVE

5.0 CONCLUSIONS AND RECOMMENDATIONS 87

5.1 Conclusion 87

5.2 Recommendation 89

REFERENCES 90

LIST OF TABLES PAGE

Table 4.1 Coordinates for extraction of Data Used in the Interpolation Programme 36

Table 4.2 Comparison Between the Bouguer Anomaly and Aeromagnetic Intensity in the Study Area 56

Table 4.11 Calculated Parameter for the Anomaly ANO1 75

Table 4.12 Calculated Parameter for the Anomaly ANO2 77

Table 4.13 Calculated Parameter for the Anomaly ANO3 79

Table 4.14 Calculated Parameter for the Anomaly ANO4 81

Table 4.15 Calculated Parameter for the Anomaly ANO5 81

Table 4.16 Calculated Parameter for the Anomaly ANO6 83

Table 4.17 Calculated Parameter for the Anomaly ANO7 85

LIST OF FIGURES

PAGE

Fig. 1.1	Generalized Geological Map of Nigeria Showing the Study Area	3
Fig 1.2	Gravity map of the Rano area	5
Fig. 2.1	Generalized Geological Map of Nigeria	9
Fig. 2.2	Geological Map of Kano State	12
Fig. 2.3	Simplified Geological Map of Nigeria	14
Fig. 3.1	Flight altitude for Resolving Anomalies at near surface	25
Fig. 3.2	Flight Plan for Aeromagnetic Survey	26
Fig. 4.2	Composite Total Intensity Map of the Study Area	32
Fig. 4.3	Total Intensity Map Superimposed on the Geological Map	35
Fig. 4.4	Distributions of Strikes of Anomaly with Azimuth Direction	37
Fig. 4.5	Regional Field Map from Robust Method	40
Fig. 4.6	Residual Map of the Study Area	41
Fig. 4.6(a)	Upward Continued Map 2 grid Units	45
Fig. 4.6(b)	Upward Continued Map 4 grid Units	46
Fig. 4.6(c)	Upward Continued Map 6 grid Units	47
Fig. 4.6(d)	Upward Continued Map 8 grid Units	48
Fig. 4.8	Autocovariance map of the study area	52
Fig. 4.9	Second vertical derivative map	55
Fig 4.10	Lineaments map of the Nigerian Basement Complex	58
Fig 4.11	Three dimensional rectangular prism	62
Fig 4.12	Residual map of the study area showing the selection of the modelling anomalies	71

Fig. 4.13 Plot of the Power spectrum of the area 73

Fig. 4.14(a,b) Observed Anomaly and Calculated ANO 01 74

Fig. 4.15 Observed Anomaly and Calculated ANO 02 76

Fig. 4.16 Observed Anomaly and Calculated ANO 03 78

Fig. 4.17 Observed Anomaly and Calculated ANO 04 80

Fig. 4.18 Observed Anomaly and Calculated ANO 05 82

Fig. 4.19 Observed Anomaly and Calculated ANO 06 84

Fig. 4.20(a,b) Observed Anomaly and Calculated ANO 07 86

CHAPTER ONE

1.0 INTRODUCTION

Magnetic prospecting, the oldest of all the geophysical survey techniques, involves the measurement of the direction, gradient and intensity of the earth's magnetic field and interpretation of variations in these quantities over the area of investigation. Anomalies are commonly related to the variations of the earth's magnetic field or contrast in the magnetic properties of the Earth materials. The successful interpretation of the magnetic variations depends largely on the existence of magnetic susceptibility contrast between the body of interest and the host rock. Most sedimentary rocks are essentially non-magnetic and thus, not amenable to direct study by magnetic methods. Igneous and metamorphic rocks generally contain a large proportion of magnetic minerals and are therefore more magnetic than sedimentary rocks.

Advancements in both instrumentation and survey techniques coupled with the development of a new field of mathematics called the Fourier transform which readily transforms data from its amplitude to its frequency form and vice-versa, has made the magnetic method to have more wider applications, both in petroleum and mining industries, as a fast way of mapping geologic structures favourable for the accumulation of ores and hydrocarbons. In the search for petroleum, the magnetic method is used for reconnaissance purpose in mapping the basement structure to determine the extent and thickness of a sedimentary sequence in a previously unexplored sedimentary basin such as the continental shelf and oceanic basins. is also used in seamount mapping and oceanography.

1.1 THE STUDY AREA

The area under study lies between the latitudes 11°00N to 12°00N and longitude 8°00E-9°00E in the administrative part of Kano State and some parts of Kaduna State in North- central Nigeria. It covers a total land mass of 12,321 km^2 Fig. 1.1 shows the location of the study area. The area is underlain by the rocks of the Nigerian Basement Complex of Precambrian to early Palaeozoic age. The Nigerian Basement Complex is believed to be as a result of at least two major orogenic cycles, (Grant, 1969; McCurry & Wright 1971). These orogenic cycles correspond to the Birrimian (2,500 my) and the Pan-African (600 ± 150 my). The earliest study of the Basement was done by Falconer (Falconer, 1911) who recognised the Pan African Older Granites and the Jurassic Younger Granites of the Jos Plateau in Central Nigeria.

The rock types of the Nigerian Basement Complex can be broadly categorized into three major lithological units (McCurry, 1970) namely:

i) a crystalline complex of migmatite and gneisses. These rocks predominate in the study area as in other parts of the Nigerian basement and they include relics of an ancient (Birrimian) metasedimentary sequence;

ii) Younger metasedimentary series occupying North-South trending synclinal belts and are usually referred to as schist belts; and

iii) a suite of intrusive syntectonic to late tectonic granites and granodiorites. These are usually referred to as the Older Granites.

The superficial deposits overlying the basement are believed to be the products of Pleistocene accumulation cycle (Wright and McCurry, 1970).

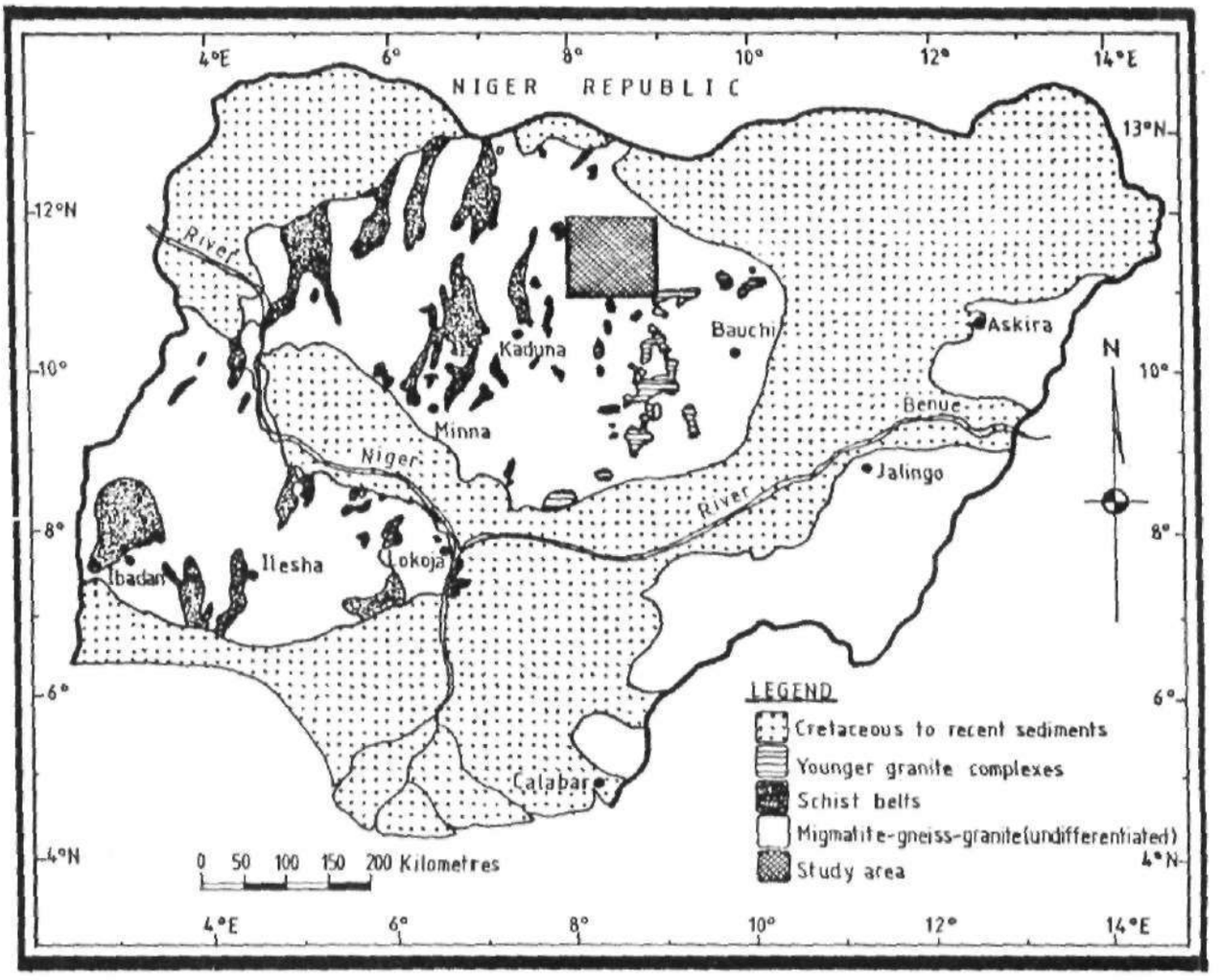


Figure 1.1. Simplified geological map of Nigeria showing the study area.

1.2 ACCESSIBILITY AND GEOGRAPHY OF THE STUDY AREA

The study area is accessible through the Kaduna to Kano dual carriage way. Some parts of the study area are also accessible through the trunk B roads, some constructed by the Directorate for food, Roads, And Rural Infrastructure (D I F R R I). The whole area is generally of low topographic relief with few granitic inselbergs and laterite mesas (Dambatta, 1990). The climate is characterized by climatic condition prevalent to the tropical Sudan Savannah,the two seasons are the dry and wet seasons. The main drainage pattern is that of River Challawa and small tributaries.

1.3 PREVIOUS GEOPHYSICAL WORK DONE

Not much geophysical work has been done in the study area. The most important work reported as far as the study area is concerned is the regional gravity survey of Kano State undertaken by Ajakaiye and Verheijen in 1977. This Work also received contribution from Gandu *et al*, (1986), Amosu (1982), Adeniyi, (1987) and Osazuwa et al ; (1992). In their preliminary report, Ajakaiye and Verheijen, (1977) reported the presence of a residual anomaly uncorrelated with predominantly granitic terrain in the Rano area. In a detailed gravity follow-up of the Rano Anomaly, Ojo *et al* (1993) show the area to be characterized by large negative Bouguer anomalies ranging from -38 mGal to -68 mGal with a mean value at -56 mgal. Several other isolated residual anomalies were also identified within the Rano Area, Fig (1.2). A prominent positive residual anomaly with amplitude of about 20 mgal was located 8 km southeast of Dal. Other smaller anomalies of both positive and negative amplitude include a gravity low with an amplitude of -6 mGal located around Sitti and Masu also another gravity low of amplitude -4 mGal is located around Gana in the north-western

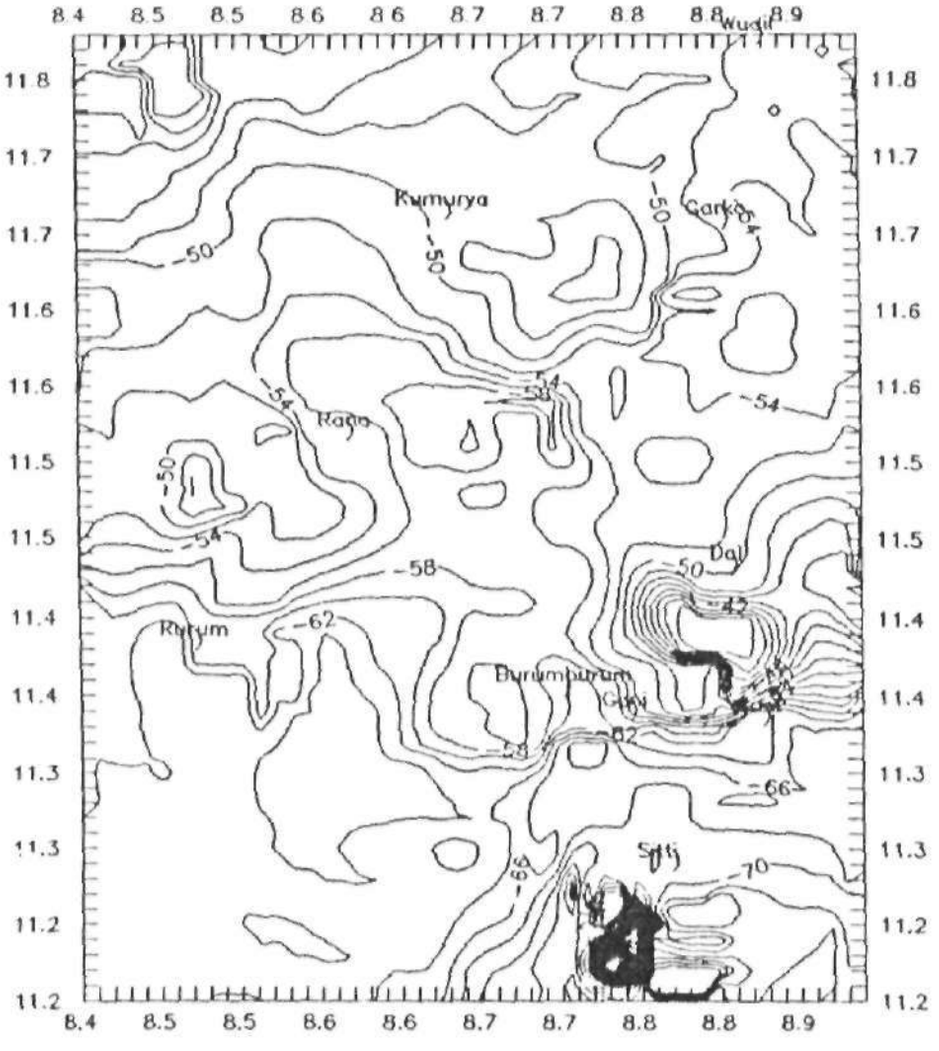


Figure 1.2: Residual Gravity Anomaly Map, Rano Area
(after Ojo et al, 1993)

part of the study area. About 5 km south-west of Karfi is a gravity high with an amplitude of about 6 mGals. The gravity lows are associated with different episode of igneous activities that lead to the emplacement of the granites whereas the gravity high are associated with high density surface at depth.

1.4 AIMS AND OBJECTIVES OF THE STUDY

As a result of the gravity Investigation in the Rano area Ojo *et al.* (1993) recommended the use of different geophysical methods to throw more light on their results. A magnetic method which is a potential field method like the gravity method is therefore used here in this study to:

ii) confirm some of the gravity anomalies identified by Ojo *et al.* (1993) in the study area;

iii) obtain additional information on the structures and the structural relationship of the rocks within this study area;

iv) investigate further the origin and mode of emplacement of the rocks within the study area;

v) identify major geological boundaries and areas of contact between the different rock units within the study area so as to provide more information to supplement the on going geological mapping of the area by the Geological Survey of Nigeria(G.S.N);

vi) carry out a 3-Dimensional modelling interpretation of some selected anomalies identified within the study area.

1.5 SCOPE OF THE STUDY

This work involve the computation of the regional and upward continuation field so as to determine the deep and regional trends. Residuals and the second vertical derivative fields will also be obtained and contoured to obtain information on the shallow to near surface bodies. The second vertical derivative obtained will also be used to delineate the geological boundaries of the different rocks units within the study area which comprise mainly the migmatite- gneiss complex and older granites (G.S.N Unpublished Geological report). The use of second vertical derivatives to delineate the contacts between the gneisses and granite units has been reported by Ali (1989), Gupta *et al* (1982), with the migmatite-gneiss showing negative intensities and the igneous intrusions showing positive intensities Alli (1989), the study will also involve statistical analysis, which consist frequency distribution similar to that carried out by Ghazala (1993) and cross-correlation of the data to establish the major structural trends within the study area. Finally, a spectral depth estimation will be done to obtain the depths to the top and bottom of the anomaly producing masses. This will be correlated with the results obtained from 3-D modelling based on the technique developed by Rao and Babu (1991).

CHAPTER TWO

GEOLOGY OF THE STUDY AREA

2.1 GENERAL GEOLOGY

2.1.0 Introduction

The Geology of Nigeria is the geology of an area which lies between the longitude 4°15′E to 14°16′E and Latitude 4°24′N to 13°6′N between the Congo and West-African cratons. About half the country land mass is overlain by the crystalline basement of Precambrian to early Palaeozoic age. The remaining half is covered by Cretaceous to recent sediments which occur mainly in sedimentary basins such as Niger Delta, Benue trough, Sokoto Basin, Chad basin, Anambra basin and Nupe Basin. The Rocks distribution over the Nigerian land mass is shown in Figure 2.1.

The Basement Complex is made up of rocks of Precambrian to early Palaeozoic age. The first study of Basement Complex was undertaken by Falconer (1911), who recognized the distinction between the Pan African Older Granites and the Jurrasic Younger Granites of the Jos Plateau in Central Nigeria.

The Nigerian Basement Complex consists mainly of six major rock groups (Rahaman, 1988),and they include the following:

i) Migmatite-gneiss-quartzite complex.

ii) Slightly migmatite to non-migmatite metasedimentary and meta-igneous rocks which are often referred to as Newer metasediments (Oyawoye, 1964), or Younger metasediments (McCurry, 1976) schist belt;

iii) Chanockitic, gabbroic and dioritic rocks.

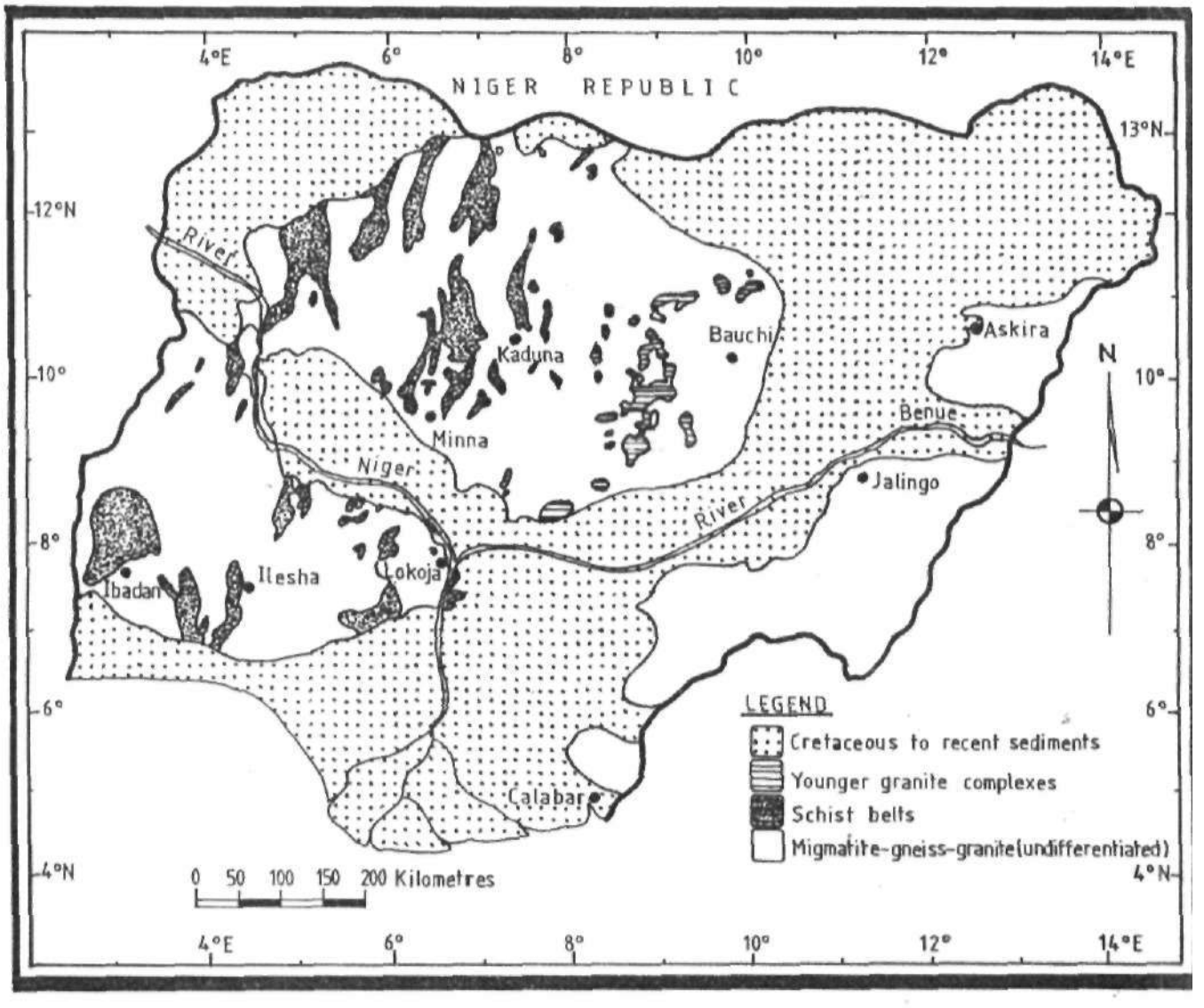


Figure 2.1. Simplified geological map of Nigeria.

iv) Members of the Older Granite suite.

v) Meta-morphosed to unmetamorphosed calc-alkaline volcanics and hypabbysal rocks (McCurry, 1976, McCurry and Wright,1977).

vi) Unmetamorphosed dolerite dykes, basic dykes and syenite dykes etc.

2.1.1 The Migmatite-Gneiss-Quartzite Complex

This group is most widespread and it occupies about 30% of the total surface of Nigeria. It is a heterogeneous rock group and comprises largely of migmatitic and granitic gneisses, basic schist and gneisses; and relict meta-sedimentary calcareous, quartzitic and granulitic rocks Rahman, (1988).

Most workers on the Nigerian Basement Complex subscribe to the view that the rocks of the migmatite-gneiss-quartzite complex comprise largely of sedimentary series associated with minor igneous rocks which have been variably altered by metamorphic, migmatitic and granitic processes. The meta-sedimentary and basic rocks are considered as relict, resisters to the migmatization and granitization processes. McCurry (1976), however, has suggested that some of these relict supracrustals may be lateral equivalents or rocks of the Birrimian system in West African craton. Other relict materials are considered to be much older and predate the granitic event of 2.8 b.y Liberian orogeny. Several problems arise from these different interpretations of the lithology within the migmatite-gneiss-quartzite complex. The first is, do the supracrustals rocks namely quartzites, amphibolites, calc-silicate rocks etc, represent a cover sequence originally unconformably overlying a basement made up of the adjacent granitic gneisses or do the gneisses represent reconstituted sediments, arkoses, grey walkers and pelite which are literally equivalent to the relict supracrustals?

A second problem relates to the question of the true origin of the quartz feldspathic gneisses. Are they metamorphosed sedimentary rocks or metamorphosed acidic to intermediate volcanics or metamorphosed granitic rocks? Rahman (1978), based on field relationship, suggested that the rocks associated with gneisses should serve as discriminant between a sedimentary or an igneous origin of these rocks. The gneisses were thus considered to be of a sedimentary origin

But a more comprehensive study of the gneisses especially the early gneiss components of the migmatite gneisses indicate an igneous origin of the bulk for early gneisses (Rahaman *et al*, 1988).

2.1.2 The Older Granites

They constituted the most obvious manifestation of the Pan-African orogeny in the Nigerian basement. They occur largely as distinct plutons often of batholithic dimensions and of limited compositional and petrographic type. Contact relationships between textural types of older granites are often complex and ambiguous. They therefore do not lead to an easy interpretation of the age relationship between the various types. Commonly, both sharp intrusive, gradational intrusive and replacive contacts exist between members of the older granite suite on the one hand and the older granites and the country rocks on the other.

2.2 LOCAL GEOLOGY

The area is part of the basement rocks of Kano State (see Figure. 2.2). and is mainly composed of migmatite-gneiss complex, the Older Granites suite, basic igneous intrusions,

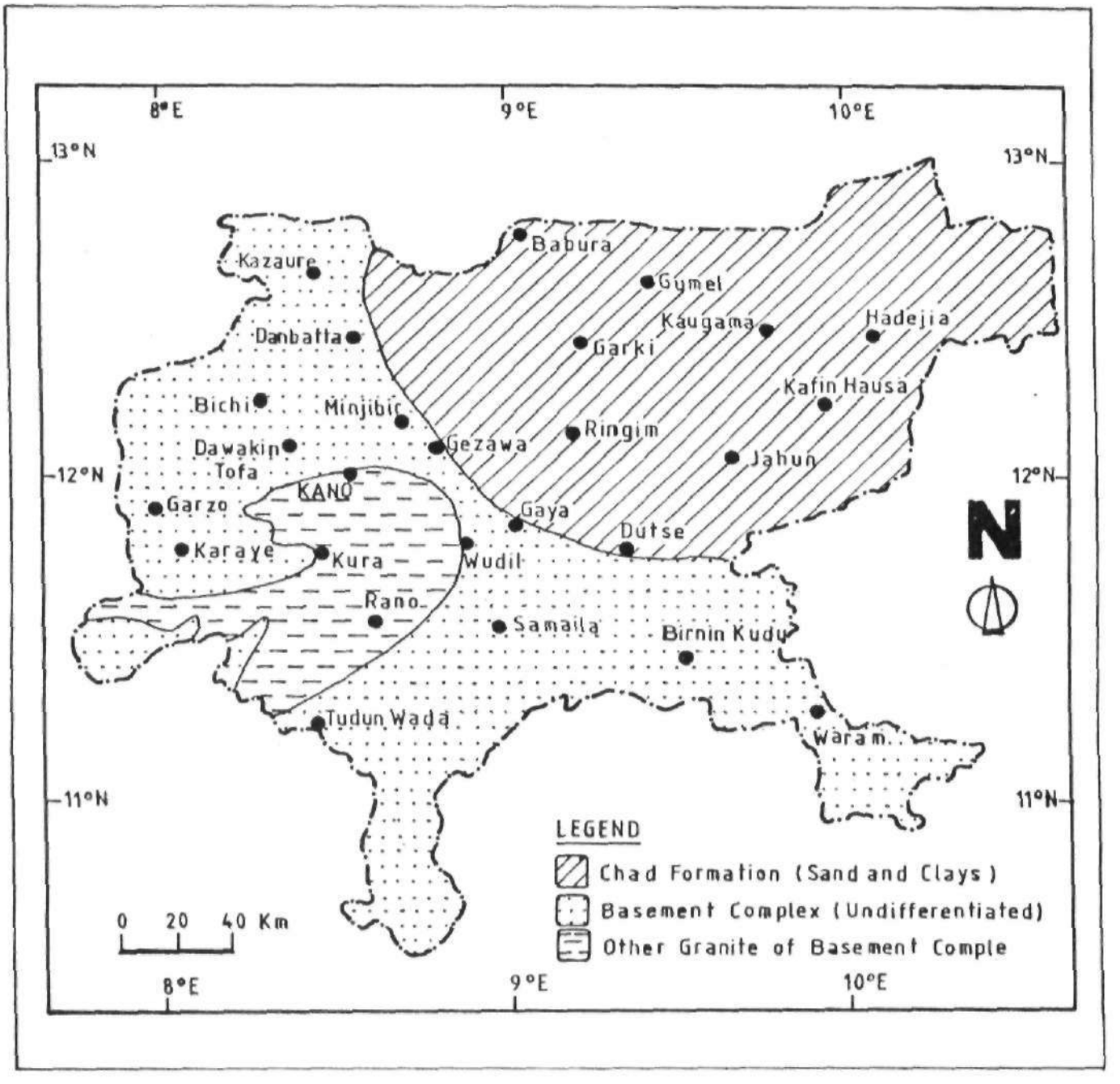


Figure 2.2. Geological map of Kano State (After Kano State Rural Intergrated Project, 1979).

and lateritic cover (Figure 2.3). The migmatite-gneiss complex includes relict quartzites and migmatites. The age of this gneisses complex is controversial but some may be as old as Liberian (2,800 my) (Ogezi, 1979). The Older Granite is composed of various types of rocks which consist of porphyritic medium and fined grained varieties. The Older Granite suite includes various types of granodiorite and basic igneous rocks (McCurry 1975), most of which are believed to be emplaced into the other rocks group about 550 my ago during the Pan-African deformation episode.

2.3 ROCK TYPES

2.3.1 Migmatites

These form subdued relief and are usually grey with bands of white and dark materials (McCurry, 1976). In some localities the dark bands prevail over the light bands while in other areas the light bands prevail over the black bands. The light bands are generally medium grained containing microcline plagioclase and quartz in neatly equal amounts. In the dark band the main feldspar appear to be plagioclase while biotite and hornblende are in greater quantity than the felsic minerals.

2.3.2 Gneisses

The gneisses vary from equiangular to porphyroyblastic in texture and are generally light to dark coloured. The major minerals in gneisses are perthitic feldspars, quartz and some plagioclase biotite and hornblende are abundant mafic minerals.

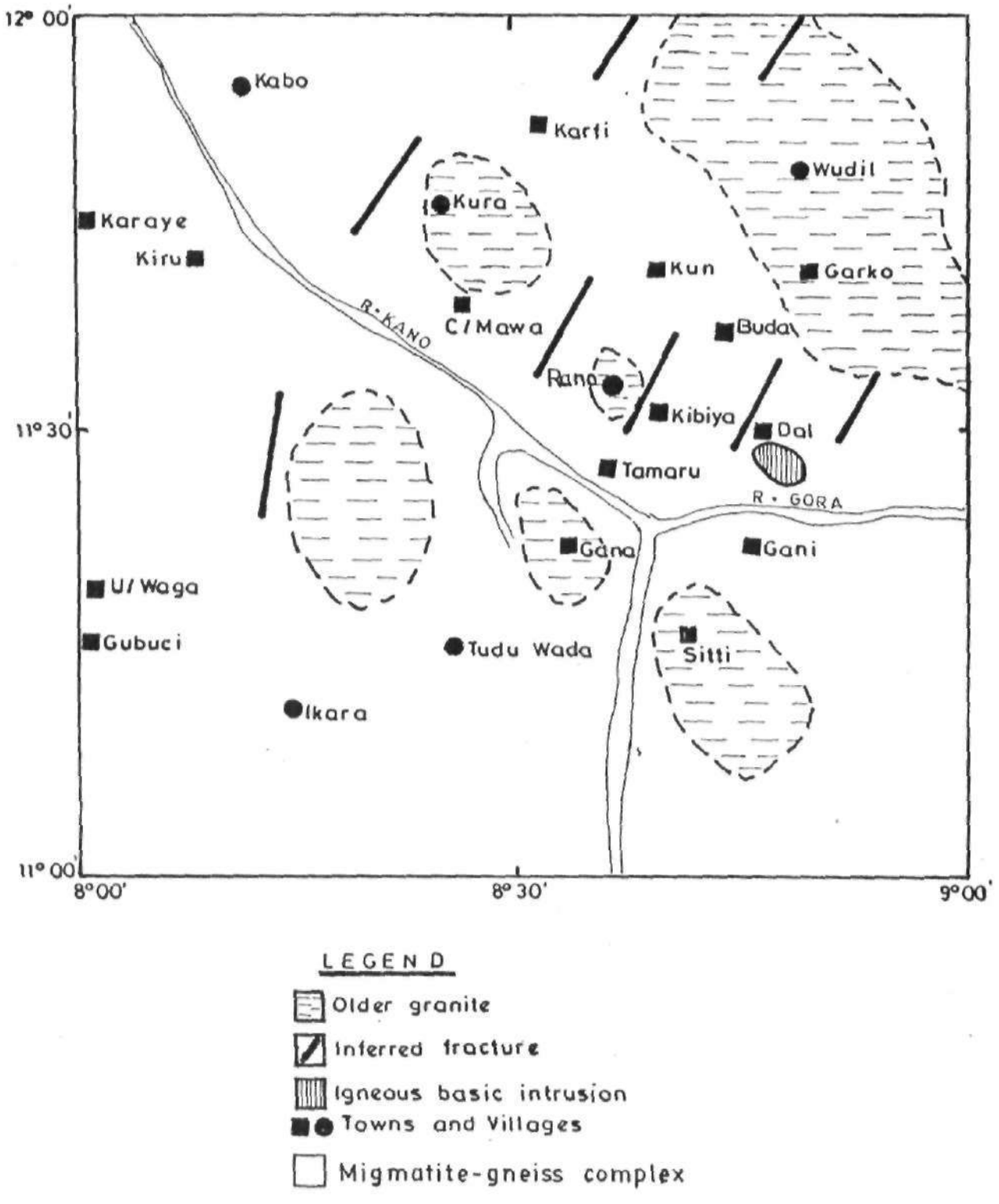


Figure 2.3. SIMPLIFIED GEOLOGICAL MAP OF THE STUDY AREA (AFTER G.S.N KADUNA AND KANO STATE RURAL INTERGATED PROJECT, 1979)

2.3.3 Granites

The granites occur in form of elliptical plutons, inselbergs and whale backs. The granites type based on texture are coarse porphyritic granites, medium-coarse grained granites and equiangular fine medium grained granites. Some of the granites exhibit some flow structures and contain rotated xenoliths indicating some movements of granitic material (Webb, 1972). The main minerals of the granites are quartz, or perthites; some sodic plagioclase with the mafic minerals are biotite and hornblende.

2.3.4 Basic Intrusives

This rock types are not very predominant as outcrops in the area probably because they are poorly exposed. One of the variety of this basic rock type, diorite is a granular rock characterized by plagioclase feldspar of oligoclase composition lacking in quartz and K-feldspar in the principal mafic minerals, but biotite is usually present with magnetite, illimenite and apatite are commonly accessory minerals (G.S.N, Unpublished Geological report).

2.3.5 Superficial Deposits

The superficial deposits are alluvial deposits and laterites, the laterites are grouped into older and younger laterites (Wright and McCurry, 1970). The former occurring prominenlyt usually along small water sheds containing quartz veins along edges of present river valleys and pediments slopes and are usually derived by erosion of older laterites. The younger laterites are partly formed insitu from weathered basement rocks and have negligible movement (G.S.N Unpublished Geological report).

2.4 STRUCTURES

There is a major North-South trend of structure in the basement with variations between the NW-SE and NE-SW. The predominantly North-South trend is due to the Pan-African event (600 ± 180 my) which affected most of the part of West Africa (Grant 1969). Some localized East-West structures also exist which are believed to be relicts of the older Pre-Pan African event (Mullan, 1978) preserved in the migmatites. The regional strike of foliations in rocks of the basement are well defined North-South trends while fold axes appear to maintain North-South trends.

2.4.1 Fractures

The principal fracture direction in the Basement Complex are the N - S; NNE - SSN, NE - SW; NNW - SSE and NW - SE and to lesser extent E - W.

CHAPTER THREE

3.0 THEORY OF THE MAGNETIC METHOD

3.1 DEFINITIONS

3.1.1 Magnetic Poles

A magnetic pole is a point near the end of a bar magnet. Poles always exist in pairs, but in a very long magnet, the lines of force around the positive pole will not be affected by the presence of the negative one. If the magnet is suspended at the centre, one end will always point in the general direction of the north pole, near this end is the North-seeking, or positive pole of the magnet near the other end is the South-seeking or negative pole. This corresponds to the South and the North pole of the earth's magnet.

3.1.2 Magnetic Force

If two poles of strength P_0 and P, respectively are separated by a distance r, the force F between them will be

$$F = \frac{1}{\mu} \frac{P_0 P}{r^2}$$

where μ is known as the permeability, which depends upon the magnetic properties of the medium in which the poles are situated.

3.1.3 Magnetic Field

The magnetic field strength at a point is defined as the force per unit pole strength which would be exerted upon a small pole of strength P_o if placed at that point. Thus the field H due to a pole strength p a distance r away is

$$H = \frac{F}{P_o} = \frac{P}{\mu r^2}$$

The unit of magnetic field is Tesla, and Tesla = 10^4Oe.

3.1.4 Magnetic Moment

The Magnetic moment is defined as the product of two pole of equal strength P and of opposite sign separated by a short distance L. Thus a magnetic moment (m) is defined as PL as the magnetic moment of dipole.

3.1.5 Intensity of Magnetization (I)

It is defined as the induced pole strength per unit area along a surface normal to the inducing field. It is also equivalent to the magnetic moment per unit volume.

3.1.6 Susceptibility

Magnetic susceptiblity is the quantity to which the degree of magnetization of a body can be measured. Magnetic susceptiblity is the fundamental parameter in magnetic prospecting, since the magnetic response of rocks and minerals is determined by the magnetic materials content in them. In the case of a homogeneous external field H which

makes an angle θ with the normal to the surface of a material capable of being magnetized, the Intensity of magnetization, I is given as

$$I = KH \cos\theta,$$

for a field normal to the surface, $\theta = 0°$, i.e $\cos\theta = 1$, thus $I = KH$, where K is known as the susceptibility. For a vacuum and completely non magnetic substance, K equal to zero. Dobrin (1982) Ferro magnetic materials have positive and relatively large susceptibilities. The interaction of the atoms and the coupling of the atomic magnetic moment in the ferromagnetic materials result in the collective behaviour of groups of atoms termed as domains. The domain orient in parallel configuration, with their long dimension in the direction of the external field, giving rise to the large susceptibility. Nearly all the studies of rock magnetism are concerned with effects of the ferromagnetic minerals. With rise in the temperature to the Curie point, the atoms decouple and the material behaves paramagnetically. Paramagnetic materials are weakly magnetic characterised by small positive susceptibility. The bulk of most rocks, for example common silicate minerals are paramagnetic or diamagnetic i.e. relatively magnetically inert. Diamagnetic substances are weakly magnetic, with negative susceptibilities. Examples of such are rock salt, are anhydride salt domes which can give rise to diamagnetic anomalies. Grains of paramagnetic and diamagnetic materials tend to line up with their long dimension acrose the external field. This effect is observed only in the presence of an external field.

3.1.7 Magnetic Induction

The field H′ which the magnetic poles induced in a material by an external field H is related to the intensity of magnetization I by the formula

$$H' = 4\pi I$$

The total magnetic flux inside the material as measured in a narrow cavity having an axis perpendicular to the field is called the magnetic induction B. This is the sum of the external and internal field and is proportional to the external field strength in moderately magnetic material as shown by the relation

$$B = H + H' = H + 4\pi I$$

$$= H + 4\pi KH$$

$$= (1 + 4\pi K)H$$

$$= \mu H \qquad (2)$$

3.1.8 Permeability

The proportionality constant $1 + 4\pi K$ is equivalent to the permeability μ introduced in equation (1) and equation (2) can thus be written as

$$\mu = \frac{B}{H} = 1 + 4\pi K \text{----(3)}$$

The permeability is a measure of the modification introduced by introduction of the forces of alteration or repulsion between two magnetic poles. Its magnitude depends on the magnetic properties of the medium in which the poles are immersed.

3.1.9 Units of Magnetic Intensity

In magnetic prospecting, one usually measures variations in the intensity or some components of the intensity of the earth's magnetic field. The conventional unit of field intensity is oersted, or its equivalent gauss. The oersted is too large a unit for practical prospecting since the interested variations are often less than a thousandth of this amount. The gamma defined as 10^{-05}Oe is more conveniently used. The gamma is equivalent to a nanotesla (nT) of the S.I. unit

3.1.10 The Geomagnetic Fields

Since the anomalies involved in the magnetic investigation are localized effects superimposed on the geomagnetic field of the earth, the knowledge and the behaviour of the geomagnetic field becomes important in both the reduction and interpretation of the magnetic field.

Nearly 90% of the Earth's field can be represented by a field of a theoretical dipole at the centre of rotation of the Earth . This field cannot in fact be said to result from a magnetism of a permanent origin in the deep interior of the Earth, the required dipolar magnetic moment are far greater than is considered realistic and the prevailing high temperatures within the Earth are far in excess of the Curie temperature of any known magnetic material. The cause of this field is attributed to a dynamo action produced by the circulation of the charged particles in coupled convective cells within the outer fluid part of the Earth's core (Elsasser, 1958). More details of the discussion on the geomagnetic field is given in Telford *et al* (1982), Dobrin (1982) and Garland (1982).

The effect due to this geomagnetic field is removed from the magnetic data using a formula known as the International Geomagnetic Reference Field (I.G.R.F) which is computed yearly. The I.G.R.F formula defines the theoretical undisturbed magnetic field at any point on the Earth surface and it is the harmonic equivalent of the Fourier analysis in spherical polar coordinates.

3.1.11 Rock Magnetization

Induced and remanant magnetization are properties related to ferrimagnetic minerals.

However, they are not governed by a simple relationship. Magnetization of rocks depends upon magnetic minerals contents, type of mineral, particle size, strength, degree of dispersion and direction of the magnetic field during the formation and subsequent changes in the earth's field. Magnetization is modified by temperature cycles, stress and stress cycle. Furthermore, tilting or rotation of block will change effective magnetization. Chemical and mechanical alteration, addition and removal of minerals and recrystallization should also cause changes.

3.2.0 INSTRUMENTS USED FOR MAGNETIC MEASUREMENTS

The most common types of portable magnetometers used for magnetic surveys are the proton-precession, alkali-vapour (or optical pumping), and flux-gate magnetometers. Other types of instruments are also used in special - purpose applications. The early magnetometers were of mechanical devices, such as field balance or dip needles, but those were replaced after the World War II by more advanced flux-gate magnetometer. The flux-gate magnetometer is in-turn, being replaced by more sensitive and less cumbersome proton magnetometer. For high precission measurement, the Alkali-vapour magnetometer would be preferred. If the magnetic relief is very small, or the object of the survey is to observed magnetic effect from sedimentary rocks that superimposed upon larger anomalies originating in the basement, the extra precission of the optical pumping magnetometer, is required. Such precision is critical in magnetic gradiometers, where the magnetic gradient is directly measured.

3.3.0 SURVEY SYSTEMS

Magnetometer surveys, are conducted on the ground, in the air, from satellites, and on ships. A ground system consist essentially of a magnetometer and some means of positioning. Airborne and shipborne are much more complex, as they require both analog and digital recording systems and other support equipment.

Airborne and marine systems can be operated as total field systems or as gradiometers. A gradiometer system measures not only the total earth's magnetic field but one or more of the earth's gradient

3.3.1 Aeromagnetic survey

The airborne magnetic survey evolved during the second world war as a way of detecting submerged submarine, coupled with radio location and other devices for locating the position of the airplane. The speed, economy and ability to pass through inaccessible terrain has lend itself as a most widely used method for magnetic survey. The Nigerian land mass has been covered by aeromagnetic surveys to aid mapping and to guide the speculation for the search for economically viable mineral resources. The survey flight was completed in July 1975 and maps were drawn in 1976. The aeromagnetic data is presented as contour maps showing points of equal strength on half degree sheets with a scale of 1:100,000 at a contour interval of 10 gamma, superimposed on the 1:100,000 topographic maps, produced by Federal Geological Survey of Nigeria;

The aeromagnetic data reflect rock distribution from the surface to the depth at which the magnetic minerals loose the ability to retain magnetization. This is caused either

as a result of high temperatures above the Curie point of the magnetic minerals or due to change in phase from solid to subliquid. In areas of high thermal gradient, the depth is usually shallow. This criterion has been used to delineate areas with high thermal gradient from aeromagnetic data (Bhattacharyya and Lue, 1975). In areas where the geothermal gradient is normal, such as cratons, the depth obtained from aeromagnetic data corresponds to the thickness of the crust.

For ore exploration aeromagnetic survey is often not too accurate, and the promising anomalies have to be confirmed by ground survey. The reason for this is that the resolution of the anomalies decrease with the flight altitude, neighbouring anomalies then overlap and smaller anomalies are lost. The anomalies lose their sharpness and detail so that it becomes impossible to separate the effect of two ore bodies at depth Y and horizontal spacing X, if the flight altitude exceeds X-Y as illustrated in Figure. 3.1. An average flight altitude for ore survey is about 150 m above terrain.

All the airborne detecting instruments measure total field, and have high sensitivities over the ground instruments (Telford *et al* 1982, Dobrin 1982; Keary and Brooks,1988). These instruments adopted for airborne survey include the fluxgate magnetometer, nuclear precession or proton magnetometer, and optical pump magnetometer. The normal precision of magnetic instruments is up to ± 1 nT. The precision normally required is approximately one part in 5×10^5 of the background field.

One problem prevalent with airborne survey is the effect of the aircraft. To overcome this effect, the sensor is towed in a housing known as `bird' 100-500ft away from the aircraft or fixed in a `stinger' in the tail of the aircraft, in which case coil installations

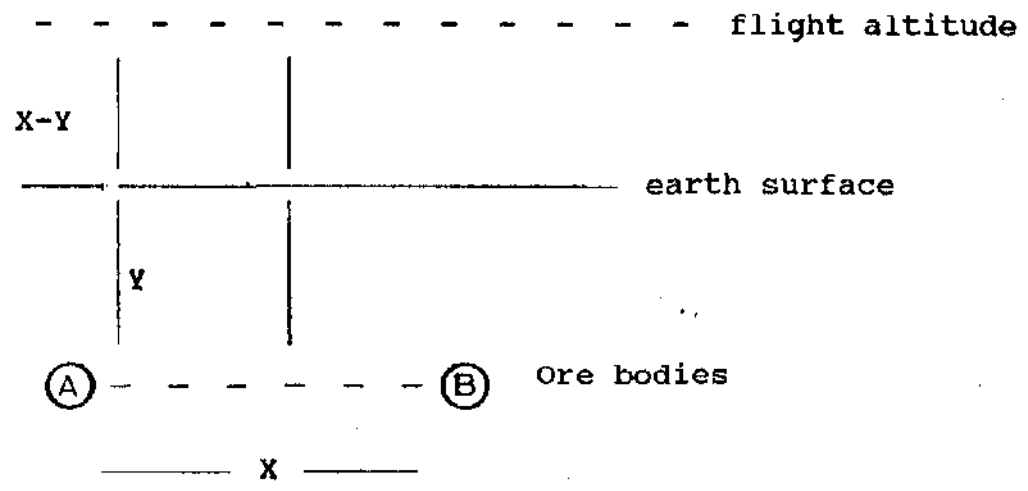


Figure.3.1 Maximum flight altitude for resolving anomalies of two neighbouring bodies. (After d'Arnound 1989)

compensate for the aircraft magnetic field. Another problem is to locate the position of the aircraft at all times with respect to the surface level. This is achieved through electronic positioning system or aerial photography.

3.3.2 Reduction of aeromagnetic data Although the speed of the aircraft has removed the effect of the instrument drift from the aeromagnetic data, the data has still to be corrected for diurnal variations. This correction is done by arranging numerous cross-over points in the survey plan as shown in the Figure 3.2. Analysis of the difference in readings at each cross-over representing the field change over a series of different time periods allows the whole survey to be corrected for diurnal variations by network adjustment. Other corrections for the aeromagnetic data includes geomagnetic and terrain corrections. More details of these are given in Telford *et al.*(1982)

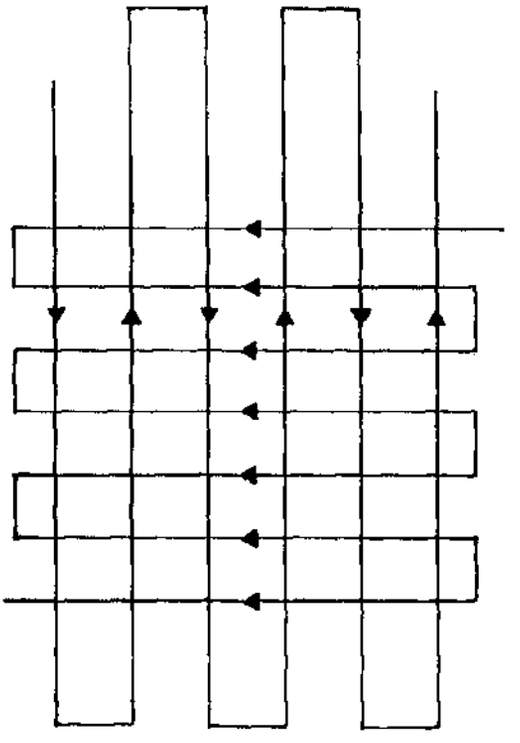


Figure 3.2. Flight Plan for an Aeromagnetic Survey (adapted from Keary and Brooks, 1988).

CHAPTER FOUR

4.00 DATA ACQUISITION, ANALYSIS AND INTERPRETATION

4.1 DATA ACQUISITION

The data used in the study were part of those collected during the airborne Geophysical Survey of Nigeria conducted by Hunting Geology and Geophysics Co. of Canada in 1975 for the Federal Government of Nigeria. The flight spacing for the survey was 2.0 km at an altitude of 150 meters above terrain. The flight line direction was NW-SE. The constructed isoline contour maps of the aeromagnetic survey was used in the study. Four aeromagnectic map sheets numbered 80, 81, 103 and 104 were obtained from the Geological Survey Division, Kaduna.

4.1.1 Data Setting

The aeromagnetic maps were digitized at the intersections of a best straight line passing through a flight line with the contours. The intersection of the contour with the flight line was considered to be the most reliable digitization procedure since it was the only point free of any human error of interpolation. At each digitizing point, two values were recorded: the contour value and the distance dl to the point of intersection. (Figure 4.1).

The coordinates of the data points were calculated in terms of longitudes and latitudes by an algorithm which converted the location of the data point from distances into coordinates given in degrees and decimal of degrees with respect to the map origin. The basis of this method was given in the diagram and the expressions below.

Consider the figure (Figure 4.1) below which was the basis for the program written for converting the longitudes and latitudes of data coordinates.

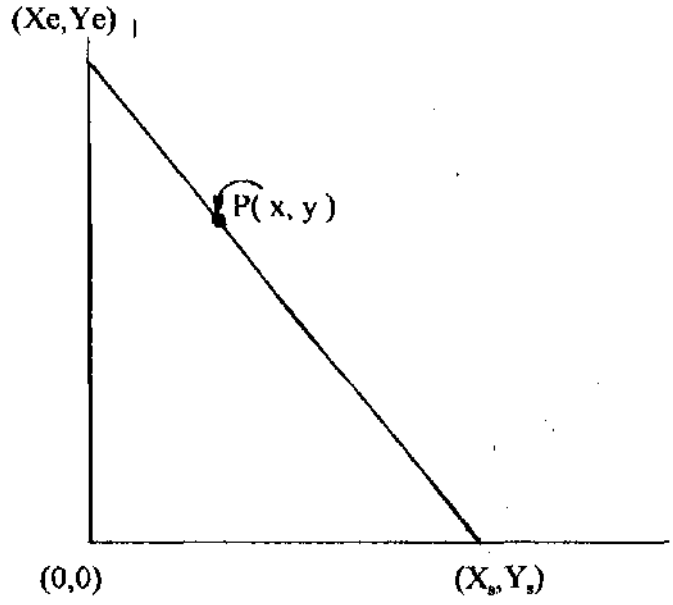


Figure 4.1: Illustration of the process of obtaining the coordinates of the data point P(X,Y).

For a point P(x, y) on the map, distance dl from the starting point of the flight line, its latitude with respect to the map origin (0, 0) is given by the relation

$$Ylp = YL\phi + [(y_s \times dl)\sin\theta] \times CF$$

and the Longitude

$$XLP = XL\phi + [(X_s - dl)\cos\theta] \times CF$$

Where (X_s,Y_s), (X_e ,Y_e) are the coordinates of the starting and end point of the flight line respectively, the angle θ is obtained by taking that.

$$\tan\theta = \left|\frac{Y_e - Y_s}{X_e - X_s}\right|$$

where Ylϕ, and Xlϕ are respectively the latitude and longitude of the map origin determined from the left most bottom corner of the map. The conversion factor CF , was the factor used for conversion from distances into degrees and decimals of degrees (CF = 0.50 / 55.3 for all the four maps). By measuring the value of dl on the map, a program (Conv.for) was written to calculate the coordinates of each data point, in terms of degrees and decimals of degree.

After digitizing, the randomly spaced data was then interpolated into a regular grid of 1.1 km by 1.1 km interval using an interpolation program written by Roland Kangkolo of Physics Department, Ahmadu Bello University, Zaria on an IBM PC/AT Computer. The program was based on the combination of least-squares interpolation and the Laplace interpolation method for interpolating randomly spaced data to a regular grid. In choosing the grid interval, consideration was given to the number of data points, size of the average anomaly of interest and the flight line spacing for which a balance was struck between these parameters.

A problem encountered during the interpolation was the size of the data with respect to the capacity of the computer which was used. Since the computer did not have enough memory to take all the data at once, the interpolation was done map by map. To interpolate for each map, a 0.05 degree search radius was allowed at each map boundary to allow for interpolation and removal of the edge effect. This was done by merging the data of one section of a map to another. This was done by extracting a data for the desired interval on each map from a combined data of all the maps which were in one data file. Thus for map 1 with original coordinates 8.00 to 8.50 and 11.00 to 11.50 the extracted data was specified

at interval 8.00 to 8.55 and 11.00 to 11.55. The intervals for extraction of the remaining maps is shown in Table 4.1.

The grided data was then combined after interpolation into one set of data by merging to remove overlap at the boundaries thus ensuring that the combined data was smooth and have no discontinuities at the boundary. The merged data was machine contoured to produce the composite total field intensity map of the study area (Figure 4.2).

4.2 ANALYSIS AND INTERPRETATION

The interpretation has been divided into qualitative and quantitative components. In the qualitative interpretation the total magnetic field intensity was contoured and the contoured map was interpreted by describing the anomaly patterns through inspection of the map. A correlation was then made between the total magnetic field map and the simplified surface geology map of the area by superimposing the Geological map on the total field map. Also, a statistical analysis to find the distribution of the strikes of the anomalies with respect to the azimuthal angle was made. In the quantitative interpretation, the total magnetic field data were analyzed for any structural trend by the method of autocovariance, (Agarwal *et al.*, 1971 and Horton *et al.*, 1984). It was then separated into its components namely the regional and residual and transformed into different types of maps for interpretation and correlation between them. These maps include the regional, the upward continuation, residual and the second derivative maps. All these analyses were done on a computer (IBM PC/AT model) of the Physics Department, Ahmadu Bello University, Zaria.

Table 4.1: Maps coordinates for which data was extracted for interpolation

	OLD MAP COORDINATES X & Y				X' AND Y'			
	X_1	X_2	Y_1	Y_2	X^1,	$X^{1\prime}$	$X^{1\prime}$	X_1,
104	8.50	9.00	11.00	11.50	8.45	8.55	11.00	11.55
080	8.00	8.50	11.50	12.00	8.00	8.55	11.45	12.00
081	8.50	9.00	11.50	12.00	8.45	9.00	11.45	12.00

X' , Y' **The coordinates at which data were extracted for each map and used for interpolation**

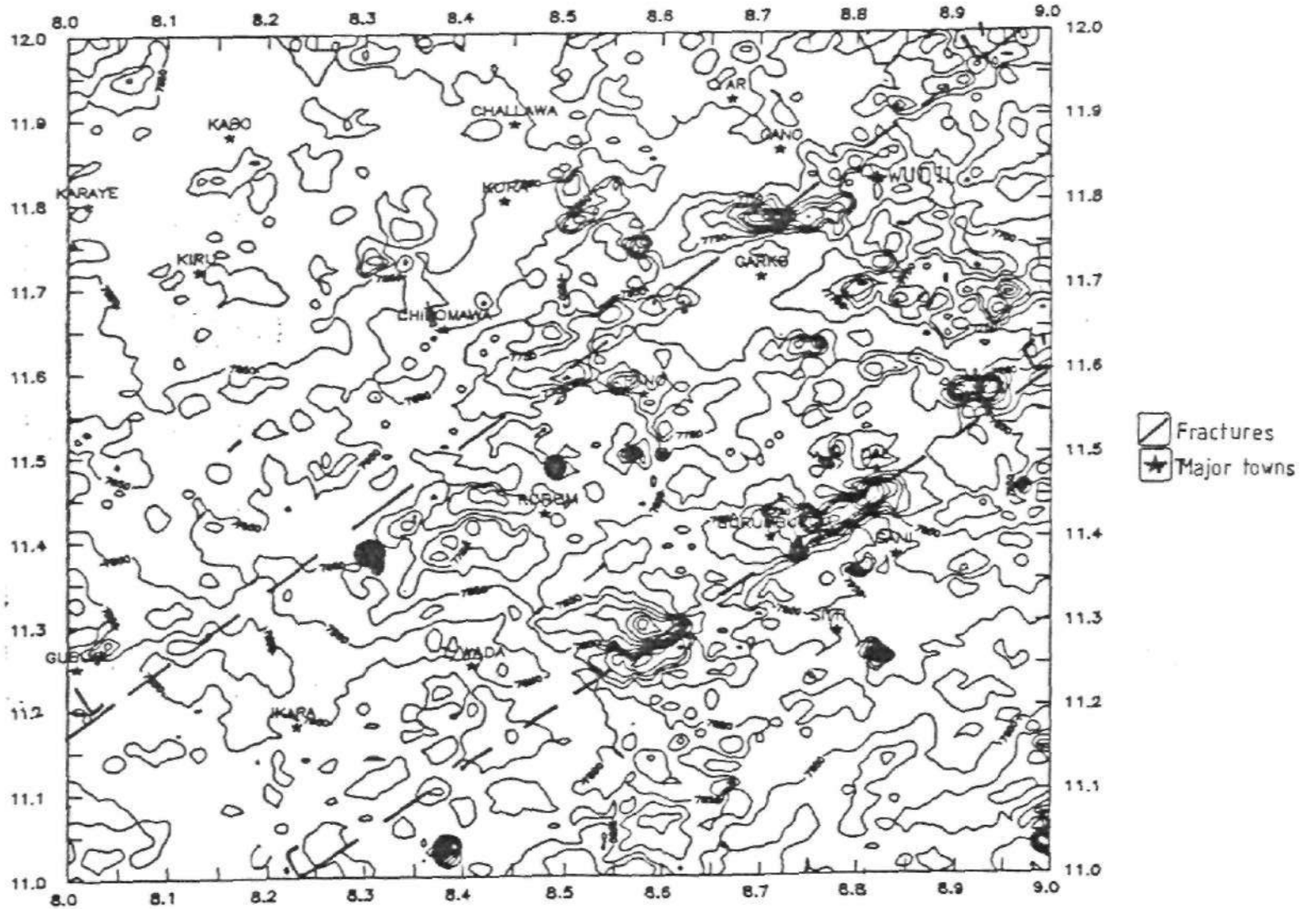


Figure 4.7. Composite total intensty map of the Study Area.

The programs were developed by Prof S.B. Ojo and Roland Kangkolo of Physics Department, A.B.U Zaria. Finally a spectral depth analysis to determine the average depth to the top and bottom layers of the anomalies and a 3-D modelling to determine the thickness and radial extent of some identified residual anomalies were carried out.

4.3 QUALITATIVE INTERPRETATION

A close inspection of the total magnetic field map (Fig. 4.2) of the study area shows prominent linear magnetic anomalies with sharp and low gradient and closures with varying amplitudes. Most of the major magnetic anomalies strike in the NE-SW direction but an E-W direction is also observed. The map can be divided into two zones: in the western part of the study area between longitude 8° 00′E to 8° 45′E and latitude 11° 00′N to 12° 00′N is the area of little or low magnetic disturbance; while in the eastern half of the study area between the longitude 8° 45′E to 9° 00′E and latitude 11°00′N to 12° 00′N starting from Burumburum to Wudil in the north, is the area characterized by many magnetic anomalies. This suggests changes in the lithology of the rocks within this area. The sharp gradients of the anomalies are believed to be due to the intrusions of magnetic bodies at shallow depth while the low gradients are due to magnetic bodies buried at greater depth in the basement. Two distinctive NE-SW trends identified as CC' and LL' on the total magnetic field map can be recognized. They suggest the presence of a magnetic lineament or shear zone crossing the study area in the ENE direction.

4.3.1 Correlation between the total field map and the geological map

Based on the available geological information, the study area may be divided into

two zones; the extreme western section of the area marked by little or no granitic intrusion, and the eastern part of the area which shows a lot of granitic intrusions surrounded by country rocks (Figure 2.3).

The geological map superimposed on the total field map (Fig 4.3) shows a good correlation between the geological and the total intensity map. It is apparent that two distinct zones shown on the geologic map are also recognizable on the aeromagnetic map. In the western half of the study area predominated by the migmatite-gneiss complex, there is little or no magnetic response, while in the eastern part of the area where there are changes in the lithology of the meta volcanics, several clusters of magnetic anomalies exist within this area. The NE-SW fractures marked on the geological map also correlate with the NE-SW Lineaments on the aeromagnetic map.

4.4 STRUCTURAL TRENDS

4.4.1 The Statistical Analysis of the Lineaments

Gay (1972) described magnetic lineaments as the disruption in the contour pattern of the magnetic anomalies, caused by juxtaposition of blocks of rocks with different magnetic susceptibility. The magnetic lineament indicates zones of weakness within the basement rocks which have undergone some displacement, and may include faults, shear zone, and contact due to intrusive and extrusive rocks.

Two methods have been adapted in the study of the lineaments; the non-orientational and orientational methods. In the non orientational method two maps, the total field map

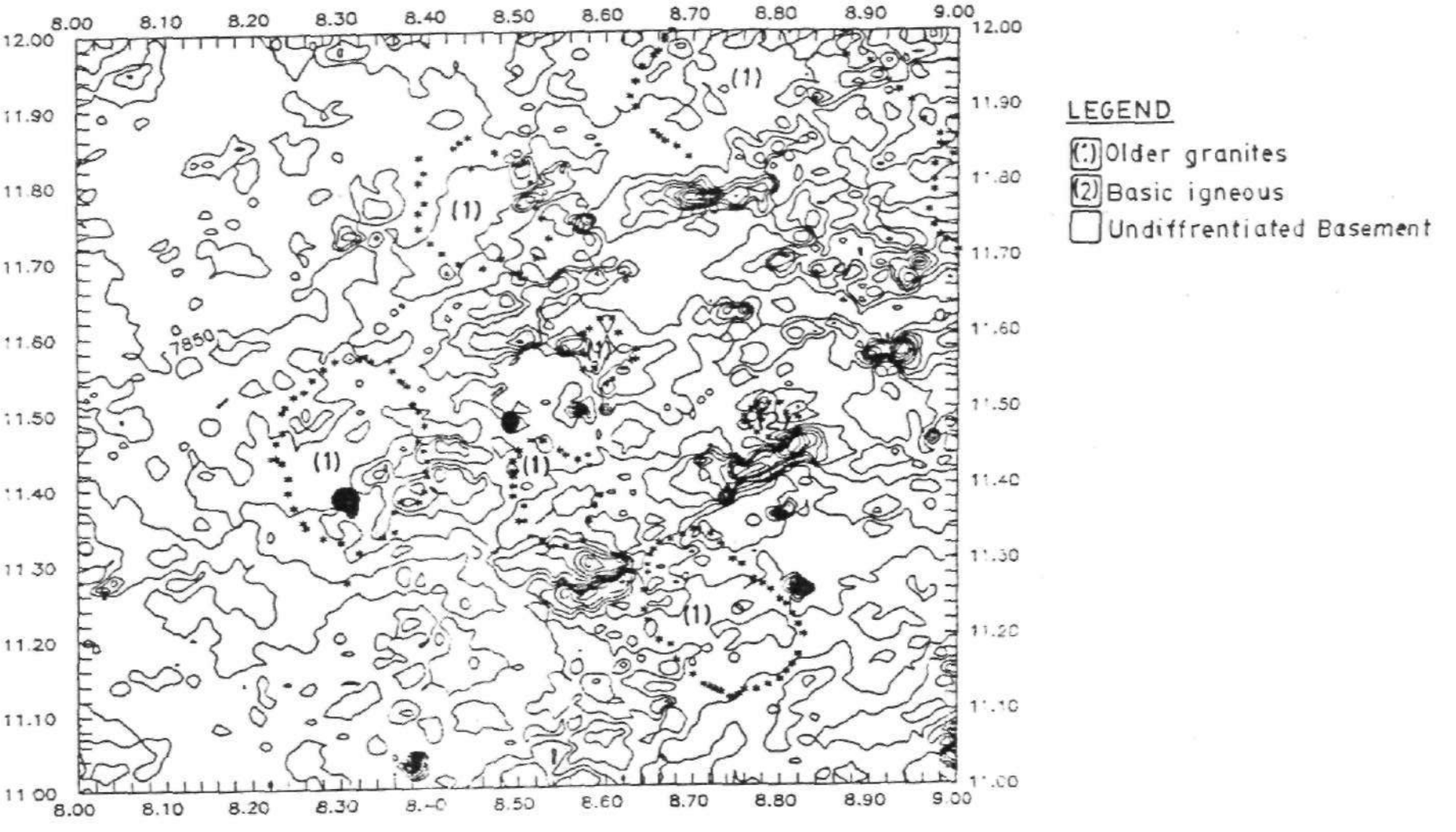


Figure 4.3. Total Field and Geological Boundaries.

and the upward continuation map were studied for lineaments using the criteria described by Gay (1972), which include the following

1. termination of magnetic lows and highs which tend to terminate against lineaments.
2. Steepening and flattening of gradient which is easily recognized from the total field, and
3. Straight patterns of magnetic contours and combination of two or more of these features.

Two trends have been recognized marked LL^1 and CC^1 from the total field map Figure (4.2) and an E-W trend in the upward continued map.

In the orientational study, the azimuthal deviations of the strikes of the anomalies was measured between 0° to 180°, the measurement was statistically grouped into classes of 10° in size and plotted on a histogram. Figure 4.4 shows a plot of frequency distribution of the anomaly strike direction with respect to the azimuth. Two peaks are notice between 50° to 60° and at 80° to 90° which correspond to the NE-SW directions which are predominant, and an E-W direction respectively. The NE-SW trend is probably attributed to the fact that the intrusive bodies causing this anomalies must have exploited the pre-existing structures during their emplacement in the basement. This view is shared by Amosu (1986) and Ajakaiye (1970). Amosu asserted that "the emplacement of granite bodies within the Nigerian Basement complex of predominantly older granite exploited the major structural displacement within the basement."

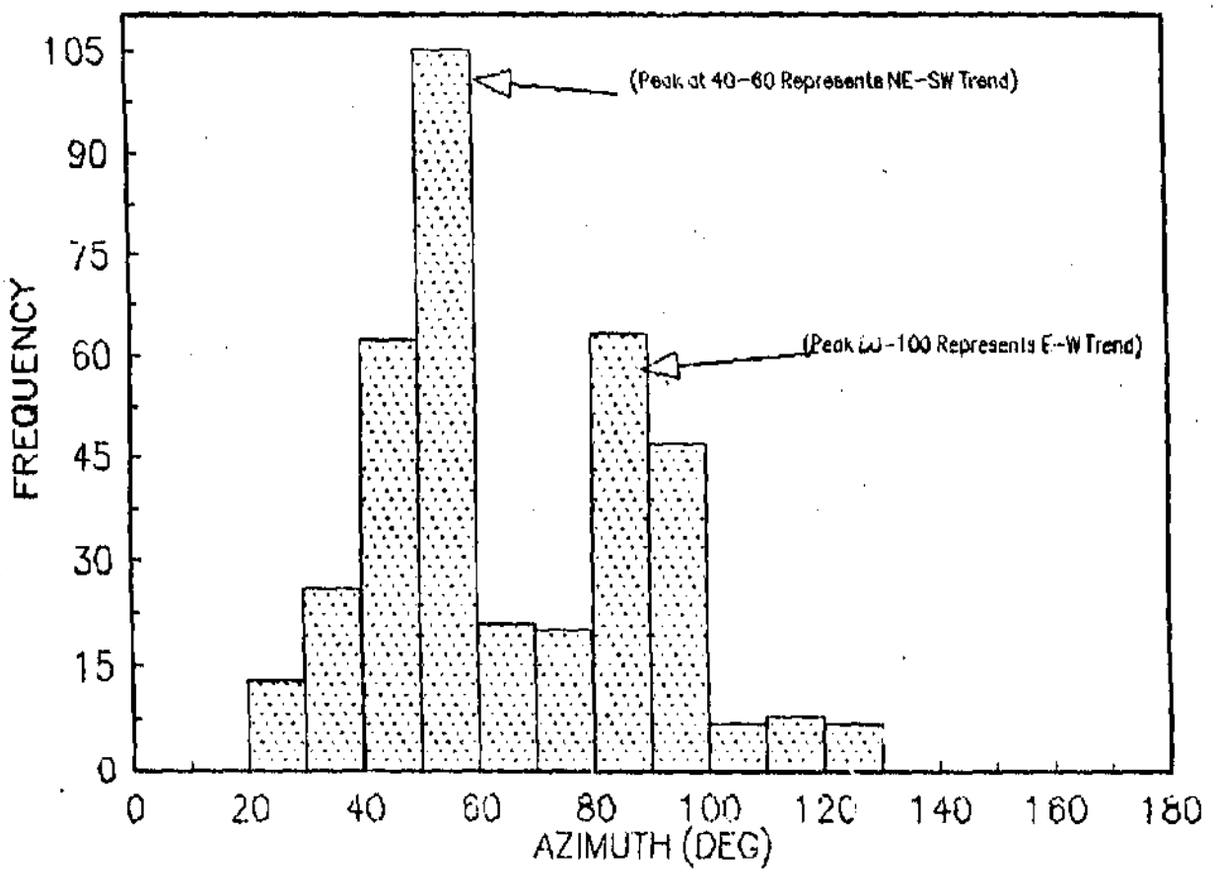


Figure 4 4. Frequency distribution of the Anomalies Strikes with Azimuth.

4.5 ANALYTICAL INTERPRETATION

4.5.1 Introduction

In the analytical interpretation the observed magnetic field data was transformed into different types of maps, namely the regional and local anomalies, 'residual' which are of economic interest; the second derivative maps,and upward continuation maps. Other analysis include the cross-correlation of the total magnetic field data to determine the structural trend, spectral analyses to estimate the average depth of the anomalies and finally, 3-D modelling to determine the thickness and radial extent of some the identified residual anomalies. Detailled description of these methods are given below:

4.5.2 Separation of Residual and Regional Anomaly

The observed magnetic field at any particular point is a vector sum of field produced by various componets. One of this which is the inner field of the earth due to basic properties of the earth, as a whole, has been discussed in section 3.1.10 and more details are given in Telford *et al* (1982), Dobrin (1982) and d'Arnoud (1989). The field has been removed from the original data based on the I.G.R.F 1974 formula (G.S.N aeromagnetic map) the remaining field contains the effect of bodies of finite dimension in the crust and large scale geologic features considerably beyond the boarders of the limited area of investigation called the regional which appears in the form of a smooth surface in the data. This was calculated by fitting a first order polynomial surface of the form T(i,j) = 7868.2-0.1122x - 62.266y to the observed data using the Robust fit method. Kangkolo (1996), also (personal communication). The computed regional was subtracted from the observed data

to obtain the field due to magnetic bodies of localized and shallow origin known as the residual field (Fig. 4.5).

The contoured regional Figure 4.6 shows an E-W trend, which confirms the result of the statistical interpretation (Section 4.4.1) This E-W trend has been recognised within the Nigerian basement complex (e.g Oluyide 1988 and Mullan 1978), it has been attributed to localized structures within the basement, which are preserved as relics; They were believed to be the oldest existing structures in the basement. Mullan 1978 was in the opinion that they were probably pre-Pan-African Origin.

4.5.3 The upward continuation of the total field

The upward continuation is carried out on a magnetic data to reduce the data to a uniform plane above the terrain, by reducing the measurement from an irregular surface Z = h(x,y) to a horizontal plane, say Z = 0, above it. The upward continuation also serves as a filter to smoothing the magnetic field by suppressing high frequency anomalies.

To a first approximation the relationship for the upward continuation can be written in form of a Taylor's series of two terms (Telford et al, 1982) as:

$$Z(x, y, z) = z(x, y, h) - h\left(\frac{dz}{\partial z}\right)_z = h$$

(i) Theoretical Basis Suppose we have a set of vertical component magnetic data z(x',y') on an irregular surface z = h(x',y'). We obtain the equivalent z(x,y) values on a plane above the surface h, say the plane z=0, z being positive downwards. Then

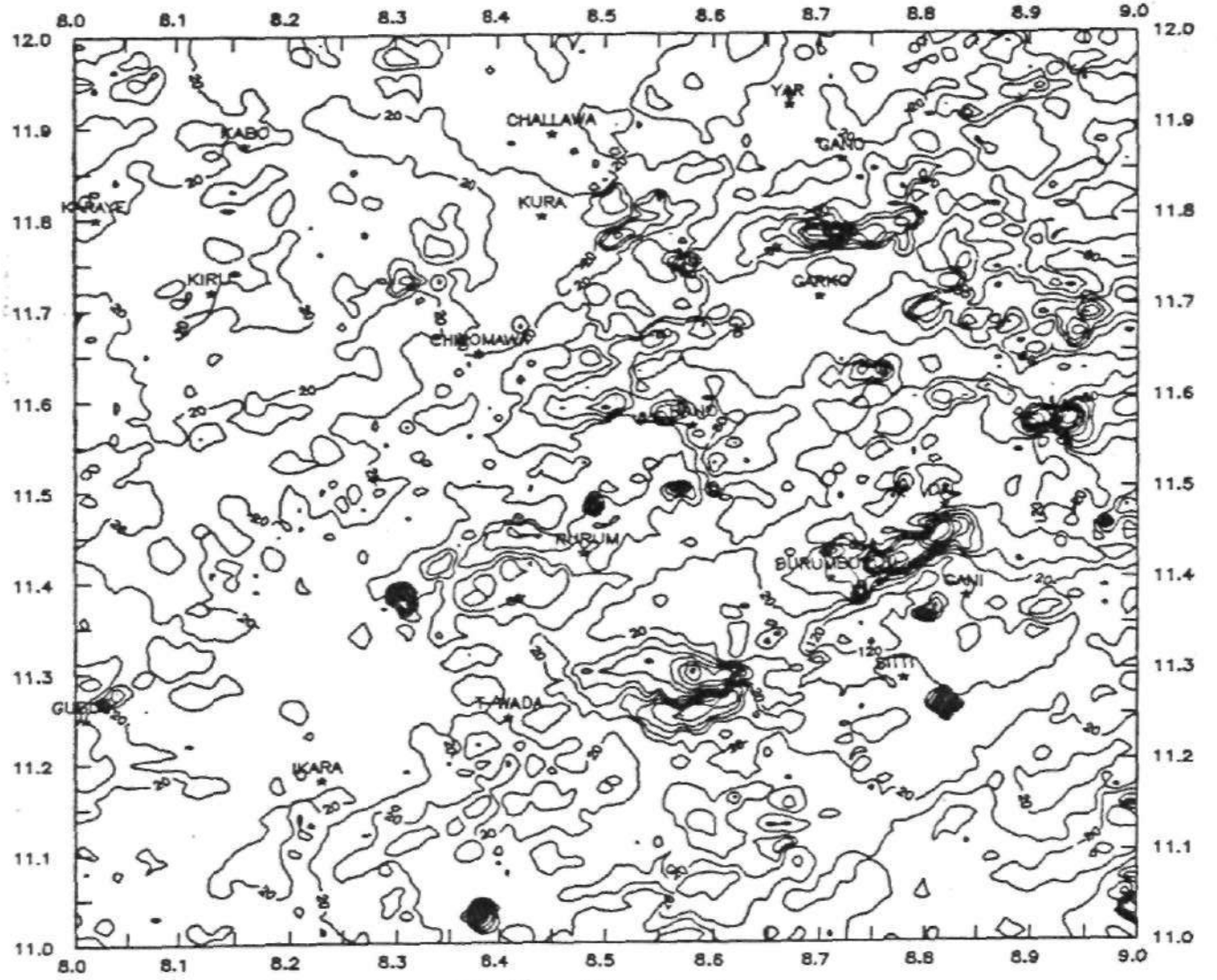


Figure 4.5. Residual Map Of The Study Area.

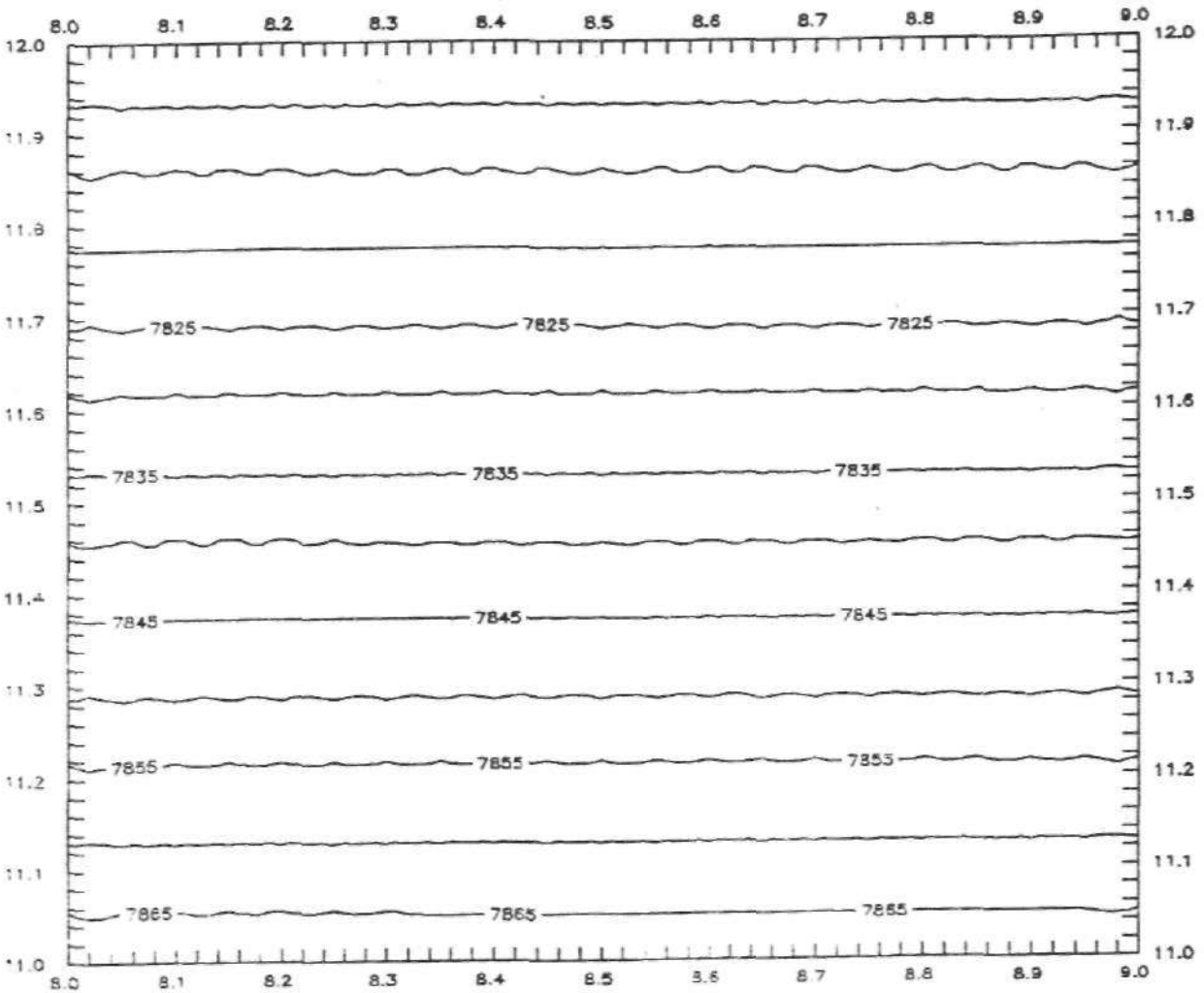


Figure 4.6. Robust Regional Field Map of the Study Area.

$$Z(x,y,z) = -\frac{1}{2\pi}\int_{-\infty}^{\infty}\int_{-\infty}^{\infty}\frac{Z(x',y')zdx'dy'}{\{(x'-x)^2+(y'-y)^2+Z^2\}^{3/2}} \qquad (1)$$

The left hand side of equation (1) is the Z value at coordinate (x,y) in a plane above or at the surface $z = h(x', y')$ on the right side. This relationship holds for all values of $Z < h(x',y')$. In polar coordinate

$$x' = r\cos\Theta$$

$$y' = r\sin\Theta \qquad (1.1)$$

If we shift the origin so that

$$x = y = 0 \qquad (1.2)$$

then from 1.1 and 1.2 above equation (1) reduces to

$$Z(x,y,z) = -\frac{1}{2\pi}\int_{0}^{\infty}\int_{0}^{2\pi}\frac{Z(r,\theta)zrdrd\theta}{(r^2+z^2)^{3/2}}$$

Since the surface for the coordinates x', y' is irregular, the conversion to plane coordinates is justified only by the use of first order approximation. Defining

$$Z(\bar{r})=\frac{1}{2\pi}\int_{0}^{\pi}Z(r,0)d0$$

as the average value of Z(r,0) around a circle of radius r, we have

$$Z(x,y,z)=-\int_{0}^{\infty}\frac{\bar{Z}(r).zr.dr}{(r^2+z^2)^{3/2}}\text{----------(3)}$$

differenciating with respect to z

$$\frac{dZ}{dz}=-\int_{0}^{\infty}\frac{Z(\bar{r})(r^2-2z^2)rdr}{(r^2+z^2)^{5/2}}$$

since Z (r) is a function of r, equation (3) can be numerically integrated to become

$$\frac{dZ}{dz}=\sum \bar{Z}(r)\int_0^{\infty}\frac{(2Z^2r-r^3)dr}{(r^2+z^2)^{5/2}}=\sum_{r=0}^{\infty}[\bar{Z}(r_n)[\frac{r_n^2}{(r_{n+1}^2+z^2)^{3/2}}-\frac{r_n^3}{(r_n^2+z^2)^{3/2}}]]$$

$$=\frac{Z(0)r_1^2}{(r_1^2+z^2)^{3/2}}-\bar{Z}(r_1)\{\frac{r_1^2}{(r_1^2+z^2)^{3/2}}-\frac{r_2^2}{(r_2^2+z^2)^{3/2}}\}$$

$$-\bar{Z}(r_2)\{\frac{r_2^2}{(r_2^2+z^2)^{3/2}}-\frac{r_3^2}{(r_3^2+z^2)^{3/2}}\}$$

If Z (0) is the measured value at a station whose coordinates on the irregular surface is (x,y,h) then

$$(\frac{dZ}{dz})_{z=h}=\frac{Z(x,y,h)}{r_1(1+h^2/r_1^2)}-\bar{Z}(r_1)\{\frac{1}{r_1(1+h^2/r_1^2)^{3/2}}-\frac{1}{r_3(1+h^2/r_2^2)^{3/2}}\}$$

$$-\bar{Z}(r_2)\{\frac{1}{r_2(1+h^2/r^2)^{3/2}}-\frac{1}{r_3(1+h^2/r_3^2)3/2}\}$$

using above expression for the vertical gradient, the values of Z(x,y,0) at any point can be evaluated at any point in the plane z=0 above the irregular surface. Using equation (1) this is

$$Z(x,y,0)=Z(x,y,h)\{1-\frac{h}{r_1(1+h^2/r_1^2)^{3/2}}\}+h[\bar{Z}(r_1)\{\frac{1}{r_1}(1+h^2/r_1^2)^{3/2}-\frac{1}{r_2(1+h^2/r_2^2)^{3/2}}\}$$

$$+\bar{Z}(r_2)\{\frac{1}{r_2(1+h^2/r^2)^{3/2}}-\frac{1}{r_3(1+h^2/r_3^2)^{3/2}}\}$$

This is obtained by drawing concentric circles around the station (x,y,h) of successively large radii r_1, r_2....r_n average the value of Z around each circle and multiply each average by the appropriate square -bracket term.

The evaluation of three dimensional case can be achieved by employing the formulae given by Henderson (1960) for the vertical magnetic component

$$Z(-h)=\sum_{i=0}^{6} Z(\bar{r}_i)k(r_i,h)$$

Z(-h) represents the vertical component at height h above Z=0. $Z(r_i)$ = average value on Z = 0 for circles of radius r_i, $k(r_i,h)$ represents the upward continuation coefficient. Henderson (1960) gives a series of coefficient values for computing Z(-h) , the coefficient method results in the distortion in the field at the map boundary due to edge effect. Tsay (1975). An alternative method is to use the fast fourier transform method.

(ii) Application and Results The computation of the upward continuation field was done via the frequency spectrum. The field is first transformed into frequency domain using the fast fourier transform. The transformed field is then multiplied by frequency domain upward continuation operator which is

$$Fu(fx,fy,h)=e^{-2\pi h(fx^2+fy^2)^{1/2}}$$

Where h represents the height of continuation and then the result is converted back into space domain.

The generation of the field was done stage by stage, by starting at a height approximately equal to twice the grid spacing, (the grid spacing equals 1.08 km) and then each time multiplying by 2. The field at a height of 2 km, 4 km, 6 km, and 8 km were generated. The results of these calculations were contoured as shown in (fig 4.7a-d). It can be seen that as the height of continuation increases the shallower anomalies are being filtered out and at height of 8km the field has become smooth. And looks more like a regional field.

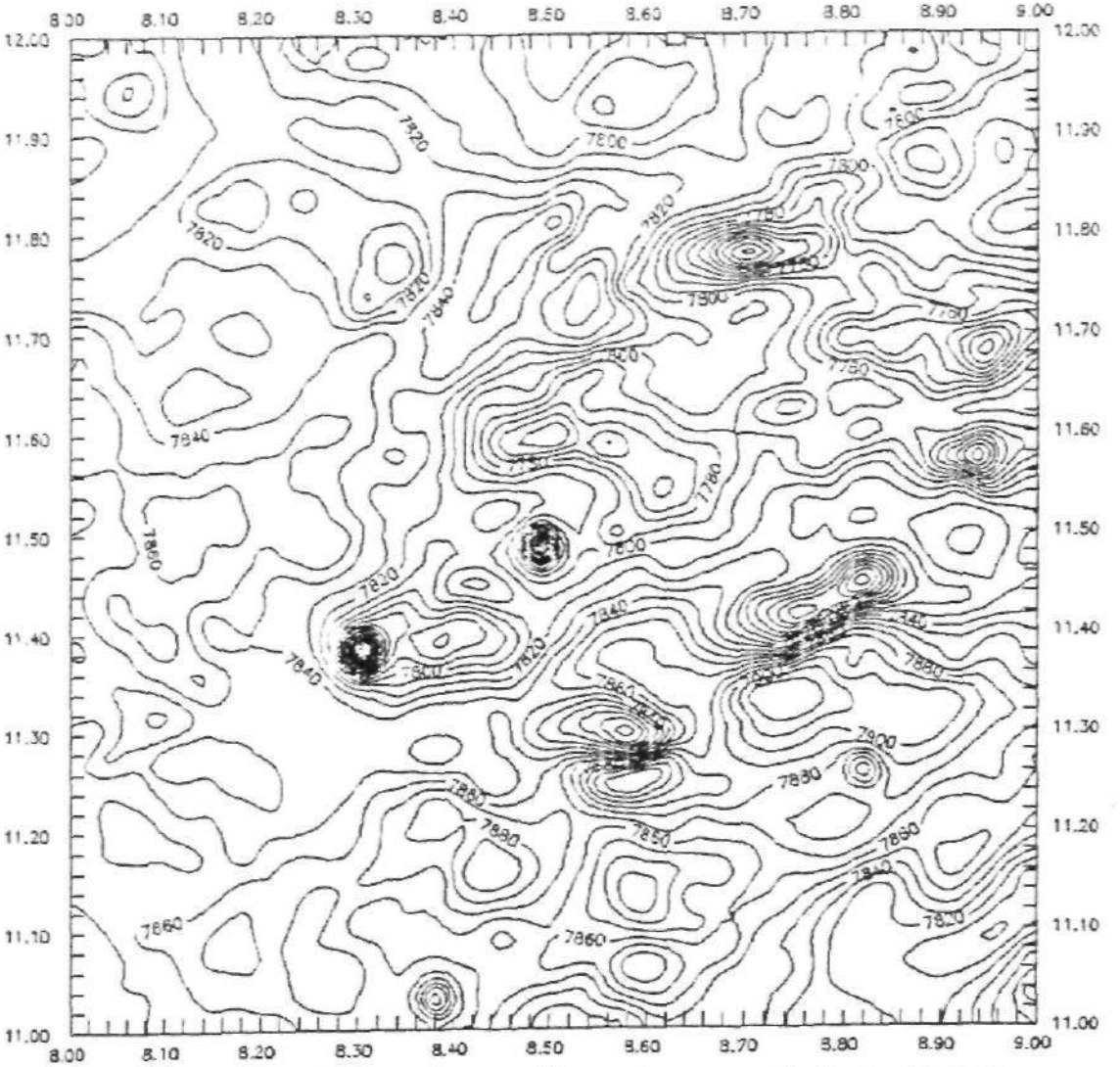


Figure 4.7a :Upward continued map 2 km above

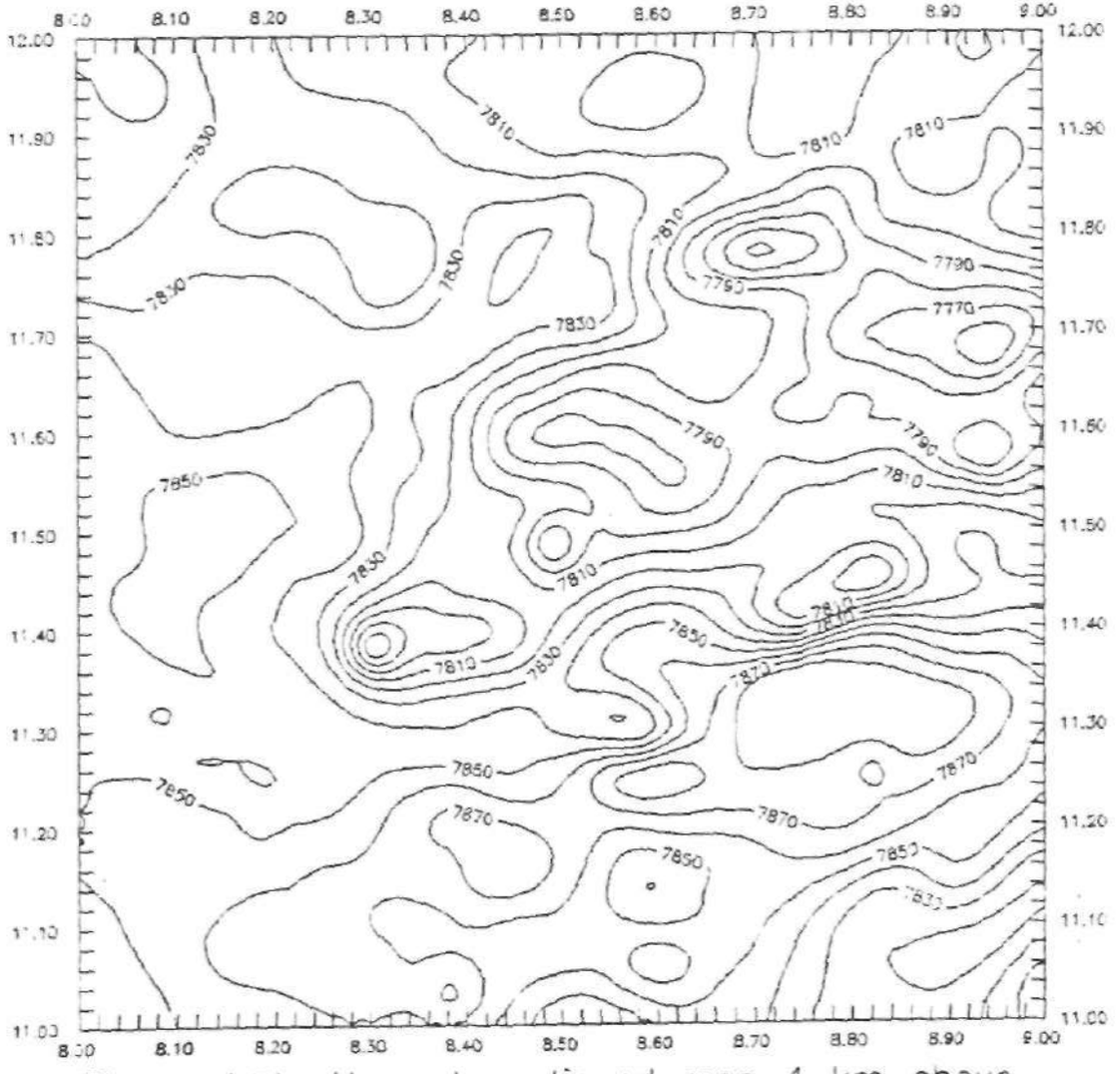


Figure 4.7b :Upward continued map 4 km above

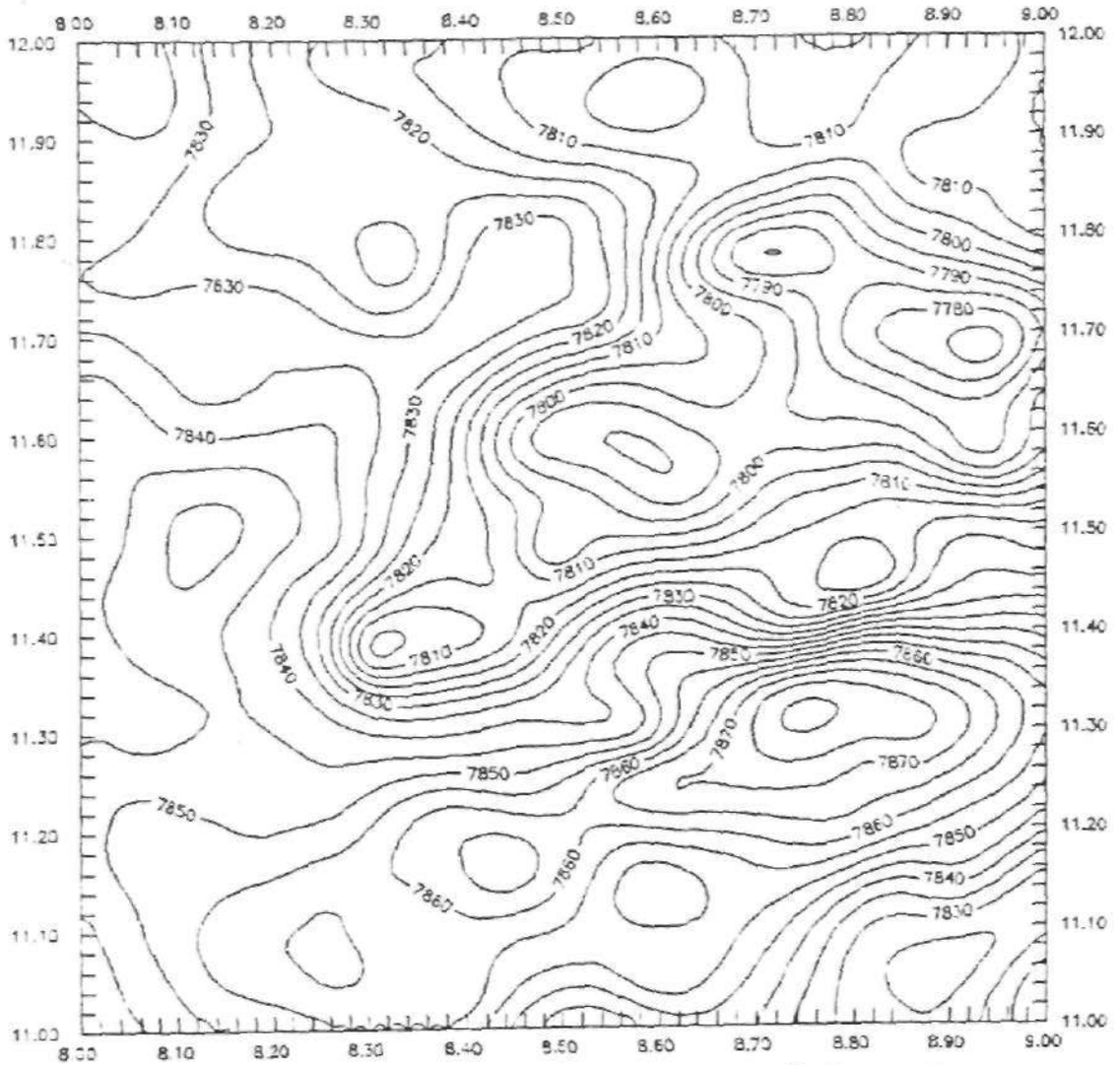


Figure 4.7c :Upward continued map 6 km above

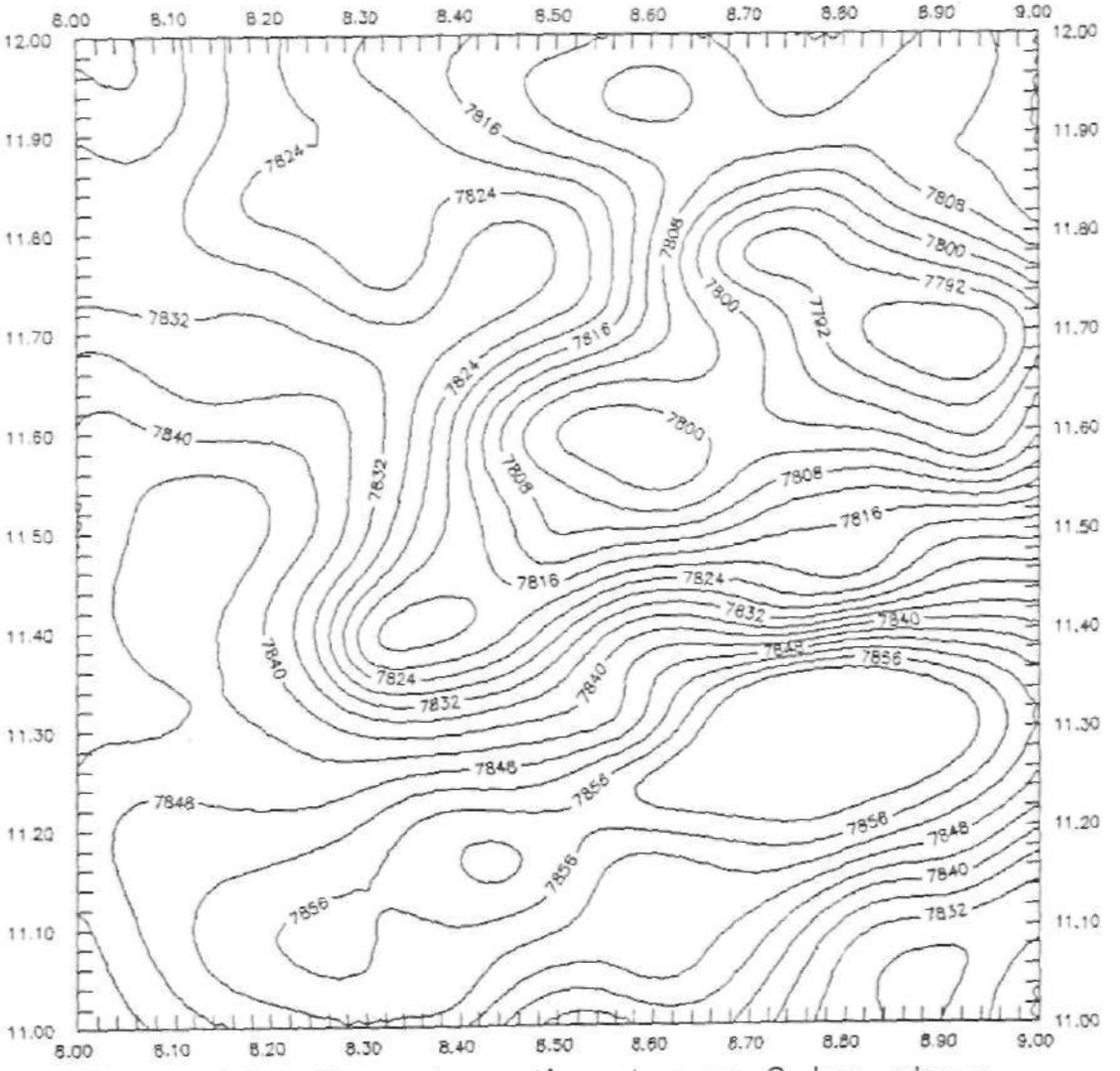


Figure 4.7d Upward continued map 8 km above

Observation of the map at height of 8 km (figure 4.7d) shows that the upward continued field has the same E-W trend which appears in the regional field (section 4.4.1). This E-W regional may have its origin beyond the area of the survey, Amosu (1986) and (Ajakaiye, 1970,1974). Ajakaiye and Verheijen (1974) have shown similar feature in the Dutse complex and the Younger Granite Province of Jos -Plateau which are to the West and East of the survey area respectively. Amosu (1986) asserted that these structures may have been the structures that were exploited during the emplacement of the granite masses in the basement complex.

4.5.4 The AutoCovariance Analysis

The aeromagnetic field is a complex phenomenon arising from more complex distribution of magnetization in the earth's crust. It therefore appears likely that the tectonic history of the rock is in some degree recorded in the magnitude and pattern of magnetic anomalies. Statistical methods can be used for the interpretation and analysis of these anomaly fields based on the concept that the magnetic field is a random function. The auto-correlation analysis has been used here for analysis of the data. The autocorrelation of magnetic data is based on the presumption that if two similar maps are placed one over the other the relationship between them will be shown. If there is this correlation, it will still be maintained if one map is slightly moved up and then displaced to the right hand-side. The theory of autocovariance of statistical data has been reviewed by Horton *et al*; (1964), Agarwal and Kanasewich (1971). The basic concept can be expressed as follows: suppose a rectangular coordinate system (x, y) is laid out on the map and Z is the quantity contoured on the map. Thus Z = Z (x, y) on the map. Assume that the calculations are restricted to

squares with sides L x L which is a sample from a larger map. Then the autocovariance function C(u,v) is defined as

$$C(u,v) = \left(\frac{1}{L^2}\right) \iint Z(x, y)\, Z(x + u, y + v)\,dx\,dy \qquad (1)$$

where the integration extends over the square $-L/2 \le x \le L/2$ and $-L/2 \le y \le +L/2$.

Autocovariance yields statistical average of all magnetic anomalies of an aeromagnetic map and can be used to interpret stress patterns in aeromagnetic maps where these trends are representative of the geologic structures creating the magnetic anomalies. The autocovariance of statistical data is determined using the following procedure: Take that the contoured map is covered by a square grid of spacing Δx and that the value of the contoured quantity at the intersection of the r^{th} and s^{th} column of the grid is Z(r,s), then equation for sample data becomes:

$$c(r,s) = \frac{1}{(N-r)(N-s)} \sum_{i=1}^{N-r} \sum_{j=1}^{N-s} z(i, j)\, z(i + r, j + S) \qquad (2)$$

$$r,s = 0,1,2.....m$$

Where m is maximum shift.

For a negative r and s, the equation is defined by c(-r, -s)= c(r,s). To complete the definition of c(r,s), c(r,-s) is defined as

$$c(r,-s) = \frac{1}{(N-r)(N-s)} \sum_{i=1}^{N-r} \sum_{j=s+1}^{N} z(i,j)\, z(i+r, j-s) \qquad (3)$$

$$r,s = 0,\ 1,\ 2\ .....m$$

Where m is maximum shift.

For ease of computation and because of their relationship with Fourier transformation and power spectrum the calculation of the coefficient of the autocorrelation was done via the frequency domain. The contoured coefficients of the Autocovariance function is shown in (Figure 4.8) This shows a structural trend tending in the ENE-WSW direction. This is in conformity with lineaments obtained with the orientational and non-orientational studies in (Section 4.4.1).

4.5.5 Second vertical derivative

A very early problem in the history of exploration geophysics was how to separate the effect of anomalies due to two bodies close together. If the bodies causing the anomalies are close relative to their distance of separation. Their anomalies will overlap, and the influence of each individual anomaly will not be seen in the single anomaly. However, If the depth decreases and the separation between the source remains the same the anomalies become narrower and appear clearly separated. This is the basis of the downward continuation method (Branov, 1975). In fact, we distinguish things more clearly when we look at them closer. However, up to the early forties, no proper computational means for the downward continuation existed and, therefore results obtained were somewhat complicated and uncertain. But it was soon realized that to obtain much more narrower anomalies without losing the trend of the original anomaly, it is easier to replace the function by their vertical derivatives. Apart from enhancing the shallower anomalies the second vertical derivative is also used to delineate contact between geological boundaries with contrast in physical properties. (Such as density and susceptibility), (Alli, S. 1989, Henderson and Zietz 1967). These contacts are reflected by inflection points in the potential field, which, while difficult

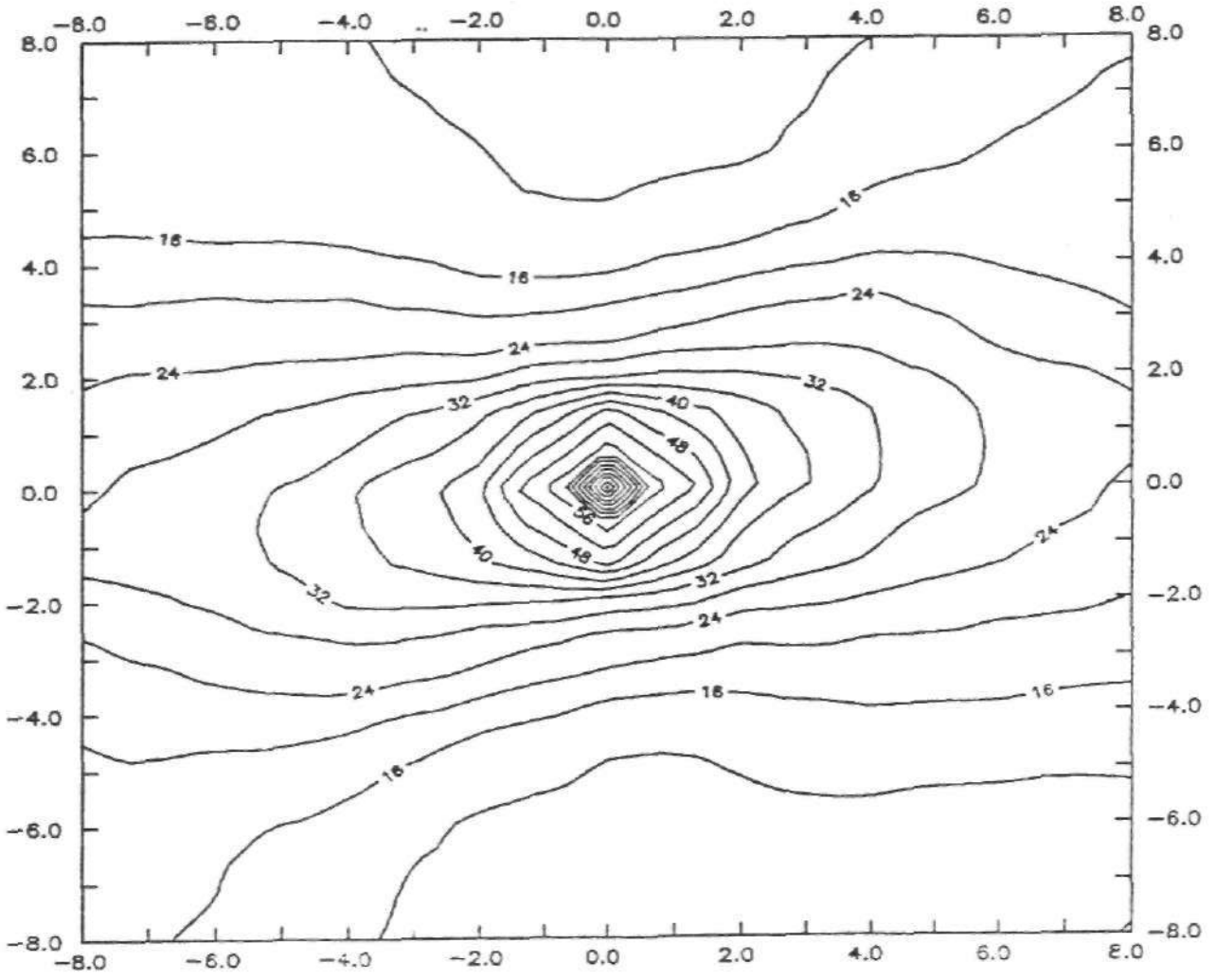


Figure 4.8.. Cross-correllogram of the total field.

to locate on the anomaly map, are accurately traced by the zero contours of the second vertical derivative map (Kangkolo, 1996).

(i) Theoretical basis: If V is the anomaly in magnetic potential at all point in free space it satisfies the Laplace equation.

$$\nabla^2 V = 0 \text{----------(1)}$$

The component of the total intensity anomaly ΔT in the direction of the earth's normal field (assumed Invariant over the area) is given by

$$\Delta T = -\frac{\partial V}{\partial z} \text{----------(2)}$$

Equation (2) is valid as long as $\Delta T << T$ where T is the magnitude of the total field. Operating on each side of the equation (2) with

$$\nabla^2 = \frac{\partial^2}{\partial x^2} + \frac{\partial^2}{\partial y^2} + \frac{\partial^2}{\partial z^2}$$

In consequence of equation (3) we have

$$\nabla^2(\Delta T) = \frac{\partial^2(\Delta T)}{\partial x^2} + \frac{\partial^2(\Delta T)}{\partial y^2} + \frac{\partial^2(\Delta T)}{\partial z^2} = 0 \text{----------(3)}$$

Therefore, ΔT on the bases assumed satisfies the Laplace equation and admits of analysis by the method of potential theory. Rearranging the equation (3) we have

$$\frac{\partial^2(\Delta T)}{\partial z^2} = -\left(\frac{\partial^2(\Delta T)}{\partial x^2} + \frac{\partial^2(\Delta T)}{\partial y^2} \right) \text{----------(4)}$$

Equation (4) is linearly dependent on the second derivatives in X and y directions. A filter can be designed to calculate the second vertical derivative. Herderson (1960) and Branov (1975), give coefficients for the computation of the second vertical derivative, but this

together with fast Fourier transform method present difficulties at the boundaries due to edge discontinuities which give distortion in the map of the transformed field (Bhattacharyya, 1972). An alternative method of calculating the second vertical derivative field is by the adaptation of spline theory (Kangkolo, 1996).

(ii) Smoothing: Since the second vertical derivative field is mostly associated with noise due to effect of bodies of very shallow origin, a filtering of the data becomes necessary. One practical method is by the upward continuation. The upward continuation operator is given by Telford et al, 1982. This equation is given by

$$F_u(u,h,v) = \exp[-2\pi h(u^2+v^2)^{\frac{1}{2}}]$$

where h is the height by which the field is continued. The upward continuation operation results in the attenuation of high frequency component of the field data, and so it can be used to filter the high frequency components before the second vertical derivative is carried out. The contoured map of the computed second vertical derivative field is shown in Figure 4.9.

(iii) Observations Examination of the contoured second vertical derivative map (Figure. 4.9) shows the map to very well correlate with the residual anomaly map Fig 4.4 The shallow anomalies appear very well in the second vertical derivative map. The gravity anomalies identified by Ojo et al (1993) are also very well reflected in the map where these anomalies are numbered 1,2,3,4 and 5 on the map.

Table 4.2 shows a comparison between the residual magnetic field and residual gravity field of the study area. It is observed that there is a correlation between the magnetic lows and the gravity high and also with gravity lows and the magnetic high. Most of these

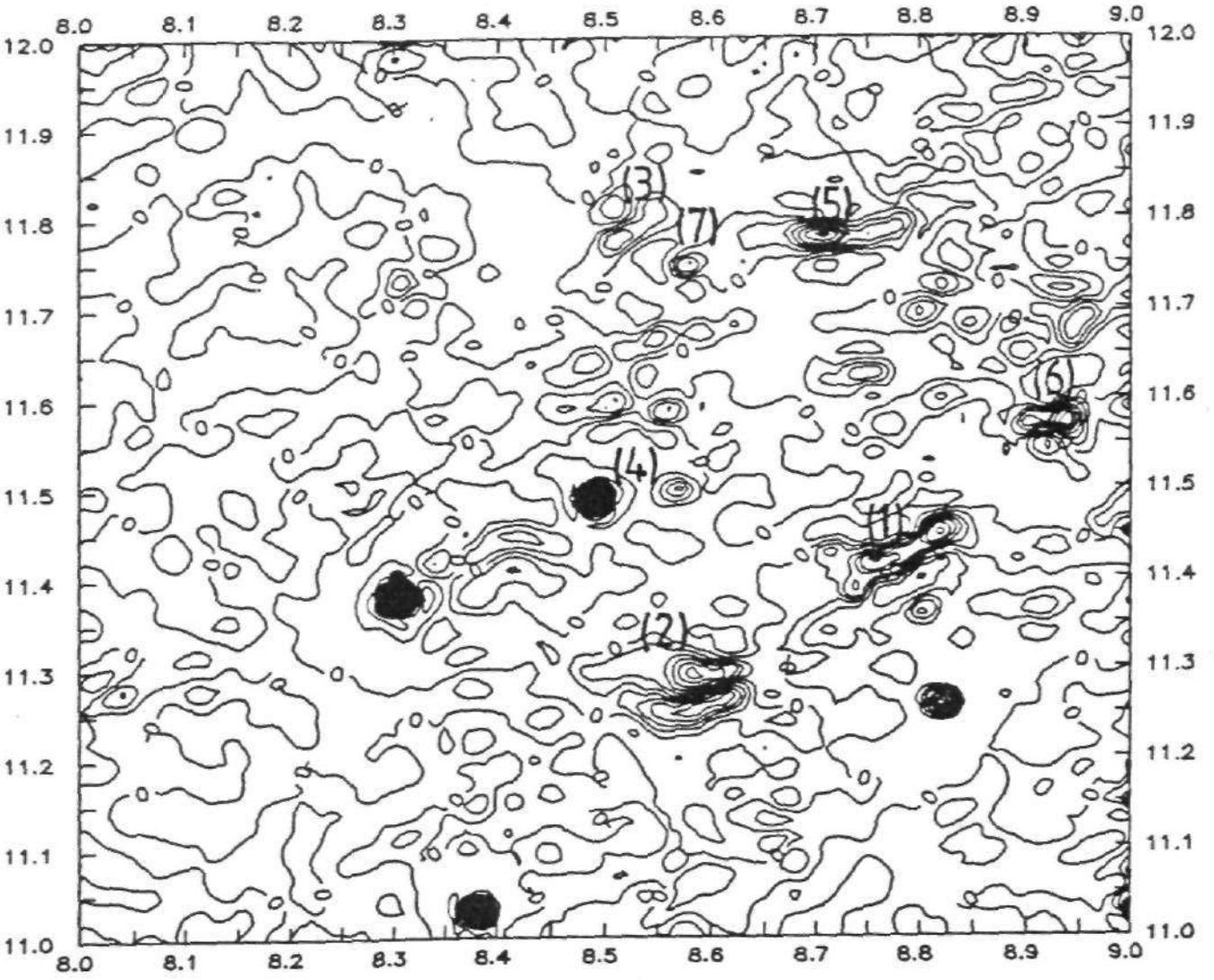


Figure 4.9. Second Vertical Derivative Map of the Study Area.

Table 4.2: Comparison between the Gravity and Magnetic Anomalies

S/No	LOCATION	LONGITUDE	LATITUDE	BOUGUER ANOMALY (g.u)	RESIDUAL ANOMALY (g.u)	AEROMAGNETIC INTENSITY (Gammas)
1	Between Gani-Dal	8.49' 0"	11.28' 27"	- 42mGal	- 16mGal	7300
2	About 8km South-East of Dal	8.46.0.	11.26.30.	-	- 5mGal	7550
3	Between Sitti-masu	8.45' 20.	11°12' 0"	- 68mGal	- 6mGal	7950
4	Around Gana	8.34.20.	11°15.0.	- 64mGal	- 4mGal	8100
5	North of Gana	8.37' 0.	11°17' 30"	-	-	7400
6	Between Garko-Kumurya	8.43' 0"	11°46' 28	- 52mGal	- 2mGal	7400
7	Near Rano	8.34.0.	11.32.0.	- 56mGal		7500
8	South-West of Garko	8.45' 0"	11°37' 0"	-	-	7600

near surface anomalies are oriented in the NE-SW direction as seen in the residual magnetic map (Figure 4.5). This suggests the presence of a sheer zone crossing this area. Elongated zero contours are also seen in the map. This reflects the different lithological boundaries with respective susceptibility contrast. This also correlates with Lithological boundaries mapped in the geological map (Figure 2.3).

4.6 GENERAL OBSERVATIONS ON THE STRUCTURAL TRENDS

A study of the structural trend, from the upward continuation, the regional and residual anomaly, the second vertical derivative and the auto-covariance analysis, has shown the major trends in the area (E-W and NE - SW trends). In summary,

i) The study area is characterised by a NE-SW residual field superimposed on E-W regional field;

ii) The correlation of the E-W regional trend with results obtained by Ajakaiye and Verheijen (1979) in the Younger Granite Complex of Jos Plateau in central Nigeria and Amosu (1986) in the Dutse complex surrounding the area confirmed their regional extent. Therefore the belief that the emplacement of the granite masses in the Nigerian Basement complex has exploited the pre-existing structure has been supported by this evidence. This evidence has shown that this emplacement which took place during the Pan African orogeny has altered the shape of the previous structures and turned them to their present shape. Relics of these structures are still preserved in the basement complex as the E-W trend. Fig 4.10 shows the major fracture trends in the Nigeria Basement complex.

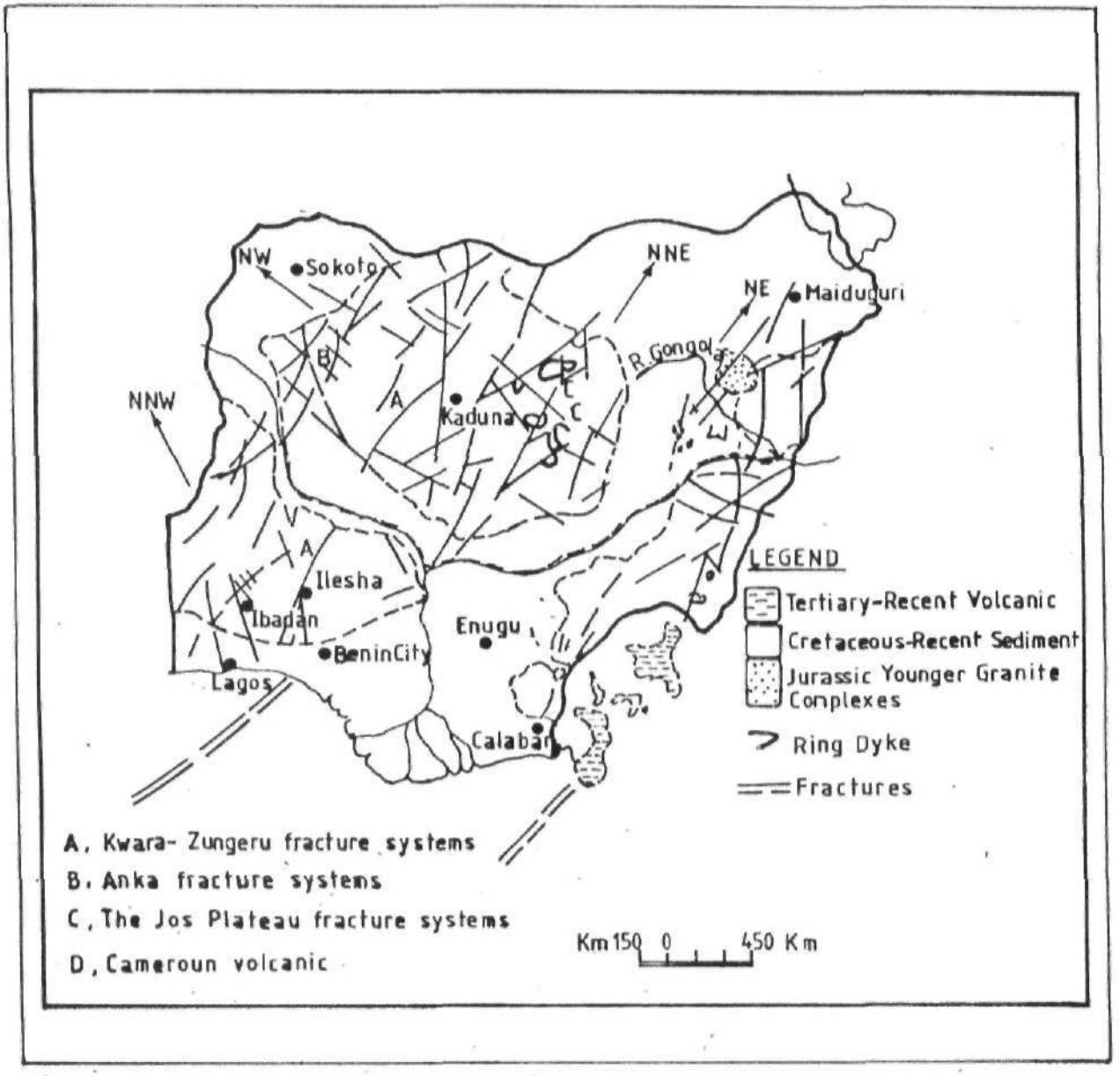


Figure 4.10. Major fracture trends in Nigerian Basement.
(After Oluyide, 1988)

4.7 THREE DIMENSIONAL MODELLING

4.7.1 Introduction

Among the most widely used models in the interpretation of magnetic anomalies is the dike, the prism and buried slopes. This interpretation which involves the determination of body parameters such as width, depth, dip and intensity of magnetization may be done using characteristic curves or by computer curve fitting techniques. Gay (1967) has reviewed the use of characteristics curves for dykes models, and Am (1972) reviewed the methods of characteristics curves for various magnetic bodies. Koulomzine *et al* (1970) developed a method which decomposes the magnetic anomaly of a dike into symmetrical and antisymmetrical parts from which parameters such as dip, centre and width of the dike model are estimated. The availability of computers has now changed the methods of interpretation in that, now, the characteristics curves are only used to get the estimate of the initial parameters which are used as inputs in further accurate interpretation by computer. The parameters are used to calculate magnetic anomalies which are then compared with the observed anomalies. If the two curves do not match, the parameters are adjusted so that the calculated curves match the observed with allowable experimental error.

Hall (1968), and McGrath and Hood (1970) suggested a technique in which the method of trial and error is used until a good fit is obtained between the observed and the calculated anomalies. This approach of iteration by which the changes of parameters is left to the interpreter to decide is subjective and time consuming and need a lot of experience. Several methods therefore have been evolved to change the parameters automatically. These

include the use of Powell algorithm for interpretation of multi-model case (Mc-Grath and Hood, 1973). Rao et al (1973) used gradient method to determine the changes in parameter vector to account for residual; Johnson (1960) used Marquardt ridge regression to optimise magnetic anomalies caused by two dimensional bodies of polynomial cross-section. Hjelt (1973) studied the performance of various methods for automatic interpretation of magnetic anomalies caused by thick sheets; Won (1981) used Gauss method to minimize the residual anomaly caused by dike like bodies.

The method being considered here is the 3-Dimensional modeling of magnetic anomalies based on the method presented by Rao and Babu (1991). This method of three dimensional interpretation of magnetic anomaly requires analysis of data over an area and assumes multiple vertical-sided prisms as a geometrical model. Structures such as intrusive plugs and uplifted basement faults are usually approximated by prismatic models. Bhattacharyya (1964) presented a closed form equation for the total magnetic field anomalies of prismatic models.

A study of aeromagnetic contour maps suggests that most of the magnetic anomalies may be interpreted as a number of magnetized bodies, which can be modeled by prismatic bodies, in general. The magnetized bodies are also closed to each other such that separation of the anomalies due to individual prism is not complete. Hence the contour map is usually interpreted using multiple prisms with different magnetization and orientations. The equation for the magnetic anomalies of a prismatic model is non-linear in its parameters, and hence many non-linear optimization techniques have been employed to interpret its parameters. Whitehill (1973) used the simplex method of interpretation of magnetic anomaly due to a single prism. Coles (1976) used Marquardt's least squares nonlinear optimization

technique to interpret magnetic anomalies due to multiple prisms. One important feature of Rao and Babu's method is its savings in computer time for the number of iterations. A non-linear optimization technique based on Marquaradt's algorithm is used to estimate all parameters of the model.

4.7.2 Anomaly Equations

Let X, Y, Z coordinates be chosen such that the x-axis points towards geographic North, the y-axis points towards the geographic East and the z-axis points vertically downwards (Fig 4.11). Let the point on the observation plane taken as the origin of the coordinates system, and the observations be taken at grid points laid parallel to the x- and y-axes. Then the equation for the total field of magnetic anomaly at any point due to a vertical prism whose sides are parallel to the coordinate axes is given by (Kunaratnam, 1981)

$$\Delta T(x,y,0) = \sum_{k=1}^{2}\sum_{l=1}^{2}\sum_{m=1}^{2} S[G_1 \ln (R_{klm} + \alpha_k) + G_2 \ln(R_{klm} + \beta_l) + G_3 \ln (R_{klm} + h_m) + G_4 \arctan \frac{\alpha_k h_m}{R_{klm}\beta_l} + G_5 \arctan \frac{\beta_l h_m}{R_{klm}\alpha_k}] \quad \text{-------- (1)}$$

Where

$$S = (-1)^{k+l+m},\ R_{klm} = (\alpha_k^2 + \beta_l^2 + h_m^2)^{\frac{1}{2}}$$
$$\alpha_k = a_k - x;\ k = 1,2 \ldots..$$
$$\beta_l = b_l - y;\ L = 1,2 \ldots..$$

and (a_k, b_l, h_m) represents the coordinates of diagonally opposite corners of the prism. The

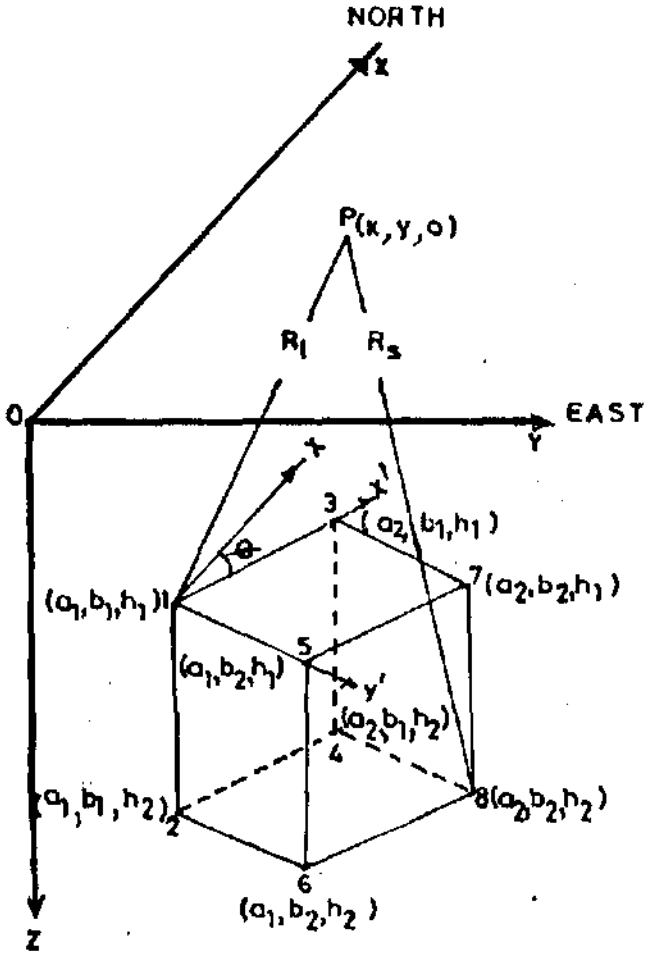


Figure 4.11. Three-dimensional rectangular prism

constants G_1, G_2, G_3, G_4, and G_5 are given by

G_1 =EI (Mr + Nq), G_2 = EI (Lr + Np)

G_3 = EI (Lq + Mp), G_4 = EI (Nr - Mq) and

G_5 = EI (Nr - Lp)

Where EI is the intensity of magnetization, l,m,n are direction cosines of magnetization, and p,q,r are the direction cosines of the geomagnetic field. If the horizontal sides of the prism are not parallel to the coordinate axis, but are rotated by an angle θ with respect to the geographic north then we have to choose a new coordinate system (x', y') parallel to the horizontal sides of the prism. The point O on the observation plane remains the origin of the New (x', y') as well as old coordinate systems, then the (x, y) coordinates in eqn (1) are to be replaced by the new coordinates (x', y') given by.

$$x' = x\cos\theta + y\sin\theta$$
$$\textit{and}$$
$$y' = -x\sin\theta + y\cos\theta$$

If I and D are the inclination and declination of the geomagnetic field, the direction cosines of the field vector are given by

$$p = \cos I \cos(D - \theta)$$
$$q = \cos I \sin(D - \theta) \qquad \textit{and} \qquad r = \sin I$$

If I_0' and D_0 ' are the inclination and declination of the magnetization vector, then its direction cosines are given by

$$L = \cos I' \cos(D' - \theta)$$
$$M = \cos I' \sin(D' - \theta) \qquad \textit{and} \qquad N = \sin I_0$$

If the observed anomalies are caused by Nb prisms, the equation for the magnetic anomaly at the field point (x, y, 0) is given by

$$\Delta T(x,y,0) = \sum_{k=1}^{Nb} \Delta T_k(x,y,0) + c \qquad \text{--------(2)}$$

where c represents a constant regional. Kunaratnam (1981) has suggested that the logarithmic terms in equation(1) can be simplified as

$$\sum_{k=1}^{2}\sum_{l=1}^{2}\sum_{m=1}^{2} S \ln\left(R_{klm} + \alpha_k\right) = \ln\left(\prod_{k,l,m}\left(R_{klm} + \alpha_k\right)\right)$$

where $\prod_{k,l,m}$ stands for the product of the function values evaluated for each k, l, and m and the arctangents in equation (1) are to be simplified using complex notation. After expansion and simplification of the logarithmic terms in equation (1)

the equation may be written as

$$\Delta T(x,y,0) = G_1 \ln F_1 + G_2 \ln F_2 + G_3 \ln F_3 + G_4 F_4 + G_5 F_5 \quad - \quad (3)$$

where $$F_1 = \frac{(R_2 + \alpha_1)(R_3 + \alpha_2)(R_5 + \alpha_1)(R_8 + \alpha_2)}{(R_1 + \alpha_1)(R_4 + \alpha_2)(R_6 + \alpha_1)(R_7 + \alpha_2)}$$

$$F_2 = \frac{(R_2 + \beta_1)(R_3 + \beta_1)(R_5 + \beta_2)(R_8 + \beta_2)}{(R_1 + \beta_1)(R_4 + \beta_1)(R_6 + \beta_2)(R_7 + \beta_2)}$$

$$F_3 = \frac{(R_2 + h_2)(R_3 + h_1)(R_5 + h_1)(R_8 + h_2)}{(R_1 + h_1)(R_4 + h_2)(R_6 + h_2)(R_7 + h_1)}$$

$$F_4 = \arctan\frac{\alpha_2 h_2}{R_8\beta_2} - \arctan\frac{\alpha_1 h_2}{R_6\beta_2} - \arctan\frac{\alpha_2 h_2}{R_4\beta_1} + \arctan\frac{\alpha_1 h_2}{R_2\beta_1} -$$

$$\arctan\frac{\alpha_2 h_1}{R_7\beta_2} + \arctan\frac{\alpha_1 h_1}{R_5\beta_2} + \arctan\frac{\alpha_2 h_1}{R_3\beta_1} - \arctan\frac{\alpha_1 h_1}{R_1\beta_1}$$

$$F_5 = \arctan\frac{\beta_2 h_2}{R_8\alpha_2} - \arctan\frac{\beta_2 h_2}{R_6\alpha_1} - \arctan\frac{\beta_1 h_2}{R_4\alpha_2} + \arctan\frac{\beta_1 h_2}{R_2\alpha_1} -$$

$$\arctan\frac{\beta_2 h_1}{R_7\alpha_2} + \arctan\frac{\beta_2 h_1}{R_5\alpha_1} + \arctan\frac{\beta_1 h_1}{R_3\alpha_2} - \arctan\frac{\beta_1 h_1}{R_1\alpha_1}$$

$$R_1 = \sqrt{\alpha_1^2 + \beta_1^2 + h_1^2}, \quad R_2 = \sqrt{\alpha_1^2 + \beta_1^2 + h_2^2}$$

$$R_3 = \sqrt{\alpha_1^2 + \beta_1^2 + h_1^2}, \quad R_4 = \sqrt{\alpha_2^2 + \beta_1^2 + h_2^2}$$

$$R_5 = \sqrt{\alpha_1^2 + \beta_2^2 + h_1^2}, \quad R_6 = \sqrt{\alpha_1^2 + \beta_2^2 + h_2^2}$$

$$R_7 = \sqrt{\alpha_2^2 + \beta_2^2 + h_1^2}, \quad R_8 = \sqrt{\alpha_2^2 + \beta_2^2 + h_2^2}$$

$$\alpha_1 = a_1 - x', \ \alpha_2 = a_2 - x', \ \beta_1 = b_1 - y' \text{ and } \beta_2 = b_2 - y'$$

4.7.3 Inversion

The magnetized prismatic body is characterized by as many as twelve parameters apart from the regional. A constant regional is assumed. Six parameters are the horizontal and vertical coordinates (a_1, a_2, b_1, b_2, and h_1, and h_2) of the prismatic body and the remaining are the intensity of magnetization (EI), the orientation of the prismatic body with respect to the geographic North (Θ), inclination (I_0), and declination (D_0) of the magnetization vector, inclination (I) and declination (D) of the earth's geomagnetic field.

Non-linear inversion techniques using Marquardt algorithm can be employed to estimate the unknown parameters. We start with an initial model and iterate on the parameters in order to minimize the objective function defined by

$$F = \sum_{i=1}^{Mx} \sum_{j=1}^{My} \left[\Delta T_{obs}(i,j) - \Delta T_{cal}(i,j)\right]^2 \quad - \quad (4)$$

where ΔT_{obs} and ΔT_{cal} are the observed and calculated anomalies, respectively, and M_x and M_y are the number of observations points in the x- and y- directions respectively.

Let the observed anomaly $\Delta T_{obs}(i,j)$ be the sum of the anomalies due to more than one prism, say Nb prisms, and let the number of unknown parameters be given by

$$N = (N_b N_p) + 1$$

including the constant regional. Then, the system of simultaneous equations becomes

$$\sum_{k=1}^{N} \sum_{i=1}^{Mx} \sum_{j=1}^{My} \frac{\partial \Delta T(i,j)}{\partial P_l} \frac{\partial \Delta T(i,j)}{\partial P_k} + \delta_{kl} \lambda dPk$$

$$= \sum_{i=1}^{Mx} \sum_{j=1}^{My} \left[\Delta T_{obs}(i,j) - \Delta T_{cal}(i,j) \right] \frac{\partial \Delta T(i,j)}{\partial P_l} \qquad - \qquad (5)$$

where l=1 to N, and δ_{kl} is Kronecker delta. Also λ is the damping factor and P_l represents one of the parameters a_1, a_2, b_1, b_2, h_1, h_2, l_0, D_0, Θ, and EI of each prism and the constant regional (C); $\partial\Delta T/\partial Pl$ represents the derivative of the anomaly with respect to P2; dI represents the increment or decrement of the k^{th} parameter to be solved for and finally to be added to the initial values of the parameters. The constant λ is to be selected by trial and error, so that the objective function decreases. Equation (5) may be written in matrix form as,

$$\underline{D} \cdot \underline{B} = \underline{P} \qquad (6)$$

In which $\underline{D}$ is the coefficient (square) matrix with known elements, $\underline{B}$ is the column matrix of unknown parameter increment to be solved for and $\underline{P}$ is the column matrix with known elements. These may be given by

$$\underline{D} = \sum_{i=1}^{Mx}\sum_{j=1}^{My} \frac{\partial \Delta T(i,j)}{\partial P_l} \frac{\partial \Delta T(i,j)}{\partial P_k} (1 + \delta_{kl}\lambda)$$

$$For \quad L = 1 \ to \ N, \quad K = 1 \ to \ N$$

$$For \quad \underline{B} = dP_k \ for \ K = 1 \ to \ N$$

$$and \quad \underline{P} = \sum_{i=1}^{Mx}\sum_{j=1}^{My} \left[\Delta T_{obs}(i,j) - \Delta T_{cal}(i,j)\right]\frac{\partial \Delta T(i,j)}{\partial P_l}$$

For l = 1 to N.

The matrix $\underline{D}$ is always symmetric and made positive definite by multiplying its diagonal elements by $(1 + \lambda)$. Hence Cholesky decomposition method (Bhattacharyya, 1980) can be used for the inversion of matrix $\underline{D}$. As the matrix D is symmetrical only the lower diagonal elements need to be calculated.

The program starts with initial values of the unknown parameters to be assumed. In the interpretation of real anomalies, the initial values of the parameters may be assumed from geological consideration and or nature of the contour map. The horizontal dimensions and the orientations of the prisms are usually assumed based on the location of the minimum and maximum closures of the contour map. In the absence of other information, the initial values for the inclination and declination of the polarization vector are assumed to be the same as the earth's field. The objective function, F_t , defined in equation (4) is found for the initial model. A value 0.5 is initially given to λ and the increment $\acute{\alpha}_{pk}$ are solved for. The partial derivatives in eqn. (5) are solved analytically by calculating the anomaly twice using equation (3) with a small perturbation in each parameter. The partial derivatives of the anomaly with respect to various unknown parameters are obtained by differentiating the

expanded version of equation (3) instead of equation (1) as it is simpler to obtain them with the former equations. Equations (5) are solved using the Cholesky decomposition method and the increments are added to the initial parameters. The objective function F_2 is again calculated using these values. If $F_2 \leq F_1$, then the step is a success and the value λ is decreased by a factor of ½ and the value of F_2 is assigned to F_1. If $F_2 > F_1$ at any stage, the search is unsuccessful. λ is doubled and equations (5) are again solved for the increments. The objective function F_2 is again calculated and compared with F_1. The procedure is repeated until $F_2 \leq F_1$. The usual convergence criterion is that the value of the objective function practically remains at the same value or the increments of various parameters are negligible.

4.7.4 Approximate equations

The computation of the magnetic anomaly and the partial derivatives at any point involves the repeated usage of equations (3), as well as its partial derivatives. The equation has been reduced to approximate equations in order to save computer time and makes programs of practical use. Approximate equations have been developed for the anomaly as well as for the initial derivatives calculation. The approximate equation for the anomaly is obtained by treating the prism as a line mass in the equation given by Kunaratnam (1981);

$$\Delta T(x,y,0) = A \int_{h_1}^{h_2} \left[G_1 \frac{\partial^2}{\partial h \partial \beta} + G_2 \frac{\partial^2}{\partial h \partial \alpha} + G_3 \frac{\partial^2}{\partial \beta \partial \alpha} - G_4 \frac{\partial^2}{\partial \beta^2} - G_5 \frac{\partial^2}{\partial \alpha} \right] \frac{1}{R} \partial h$$

Where

$$R = \sqrt{\alpha^2 + \beta^2 + h^2} \qquad and \qquad A = (a_2 - a_1)(b_2 - b_1)$$

Integrating the right hand side of this equation with respect h. This equation becomes.

$$\Delta I(x,y,0) = A[(G_1\beta + G_2\alpha)\left(\frac{1}{R_1^3} + \frac{1}{R_2^3}\right) + G_3 C_1 \frac{\alpha\beta}{\alpha^2 + \beta^2} - G_4 \frac{(C_1\beta^2 + C_2)}{x^2 + \beta^2} - G_5 \frac{(C_3\alpha^2 + C_2)}{x^2 + \beta^2}] \qquad (7)$$

where

$$\alpha = \frac{a_1 + a_2}{2} - x', \quad \beta = \frac{b_1 + b_2}{2} - y'$$

$$R_1 = \sqrt{\alpha^2 + \beta^2 + h_1^2}, \quad R_2 = \sqrt{\alpha^2 + \beta^2 + h_2^2}$$

$$C_2 = \left[\frac{h_1}{R_1} - \frac{h_2}{R_2}\right] \quad and \quad C_1 = \left[\frac{h_2}{R_2^3} - \frac{h_1}{R_1^3} - \frac{2C_2}{(\alpha^2 + \beta^2)}\right]$$

This equation is valid at all points except in the range defined by

$(a_2 + 2) > x > (a_1 - 2)$ and $(b_2 + 2) > y > (b_1 - 2)$

where a_1, a_2, b_1 and b_2 are given in grid units. Similarly approximate equations for the partial derivatives are obtained by differentiating equation (7) with respect to various parameters.

The use of the exact and approximate equations may be efficiently monitored as a trade-off between accuracy and speed. Thus, for the first few iterations where accuracy is less important, the approximate equations are used to calculate the anomalies and the derivatives at all points except in the region defined by the horizontal projection of the prism on the observation plane and the immediate two neighbouring points from the boundary of the horizontal projection. As the iteration progresses, the exact equations are used for calculating the anomaly on the top and more neighbouring points of the prism.

4.8 THE PRESENT APPLICATION

The anomalies that were modeled using the above method were identified from the second vertical derivative map (fig 4.9),and are also shown on the residual map (fig 4.5). Seven anomalies were selected and extracted within the study area (fig 4.12). Five of these anomalies correspond to the gravity anomalies identified by Ojo *et al* (1993), while the others were not identified in the gravity survey due to problems of road accessibility. The anomalies are numbered ANO 01 to 07. The residual fields of the anomalies were modeled.

4.8.1 Initial parameters

The convergence of the algorithm to obtain a realistic model depend on the choice of good starting values for the model parameters. Initial parameters of the anomaly models were assumed from the study of the geological map of the area and the average depth results obtained from spectral analysis. In the case where a particular anomaly outcrops on the geological map the depth to the top of the anomaly is assumed to reduce zero and the depth to the bottom was estimated from spectral analysis. Two blocks of 64 km x 64 km

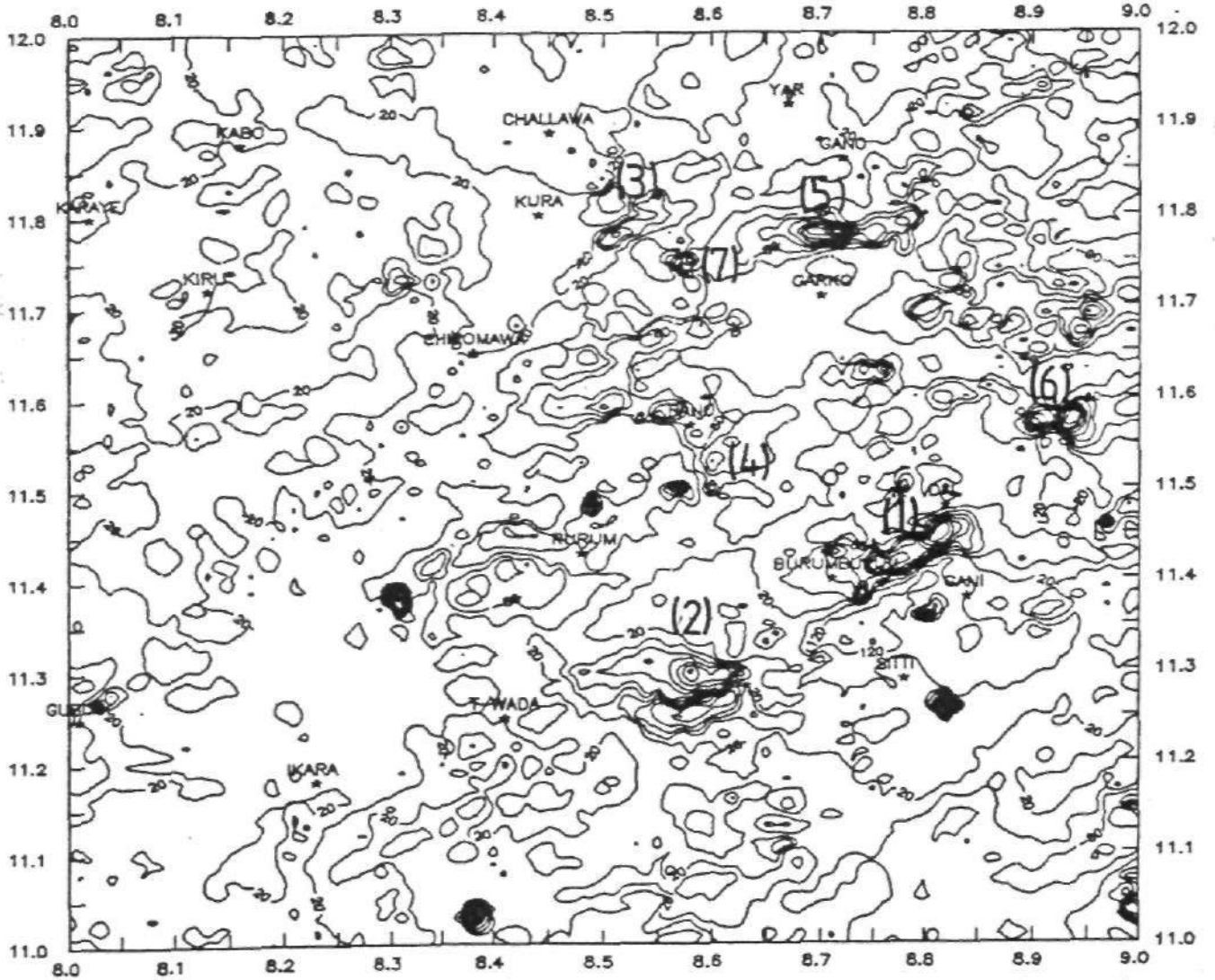


Figure 4.12.Residual Map Of The Study Area .and Selected Anomalies .

which overlap were selected in the study area. The plot of the power spectrum versus frequency of the two blocks shows two depth segment in which a straight line could be fitted (fig 4.13). The first segment corresponds to the deepest source and the average depth range from 5.2 km to 6.8 km. The second segment represent depth of shallow source and range from 0.45 to 0.65 km. The inclination, declination and the total field intensity of the earth were obtained from the lines crossing the area on the earth plots of the parameters, the initial geometric parameters of the modeled bodies were measured on the individual anomaly map. Figure 4.13 shows the plot of this parameters with respect to the rotated system. The interpretation of the individual anomalies is discussed below. The values of the susceptibility contrast given are in cgs units to obtain SI units values are multiplied by $4\prod$.

4.8.2 Anomaly number ANO 01

This anomaly is centred around Gani about 8 km south east of Dal between the latitude 11.36°N to 11.48°N and longitude 8.69°E to 8.85°E. The anomaly is a magnetic low of amplitude about -320 nT with strike trending in the NE - SW direction. The anomaly occurs over an outcrop in the geological map and correlates with a not so prominent basic igneous rock in the study area. The shape of the anomaly is shown in Fig 4.14a and the interpreted model shown in Fig 4.14b.

The anomaly has been interpreted to be composed of four prismatic bodies. After the 20th iteration the objective function reduced from 2,960,248.0 to 523,966.2 with a percentage correlation between the observed and calculated field being 92.8% A constant regional of 4.86 nT is found in the area. The interpreted parameters of the anomaly corrected for flight elevation are given in Table 4.11.

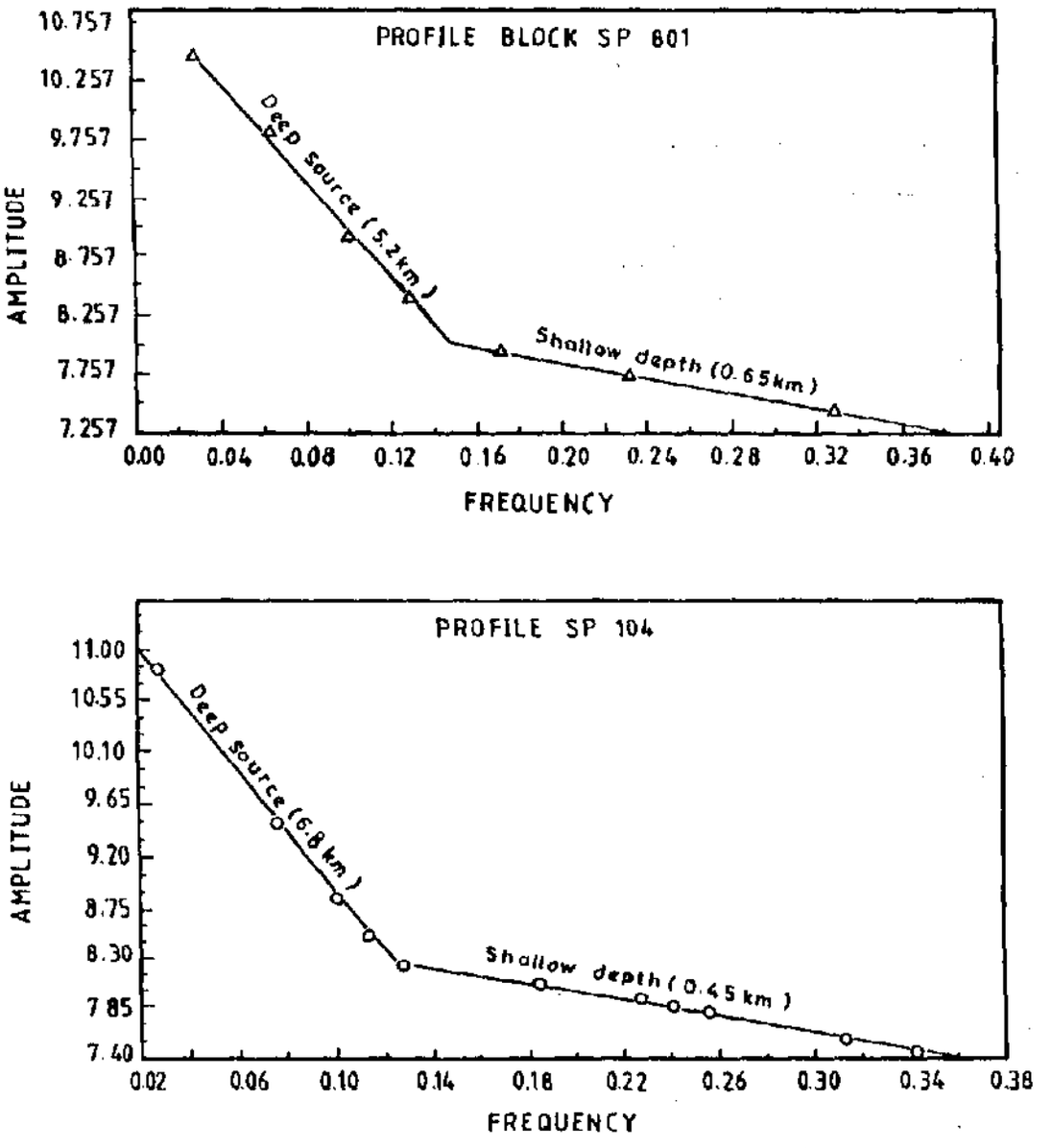


Figure 4.13. Spectral amplitude of two blocks within the study area.

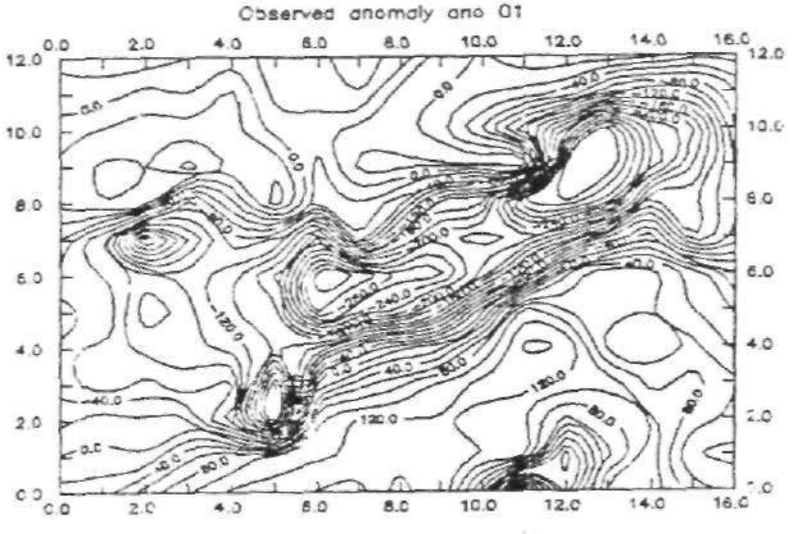


Figure 4.14(a).

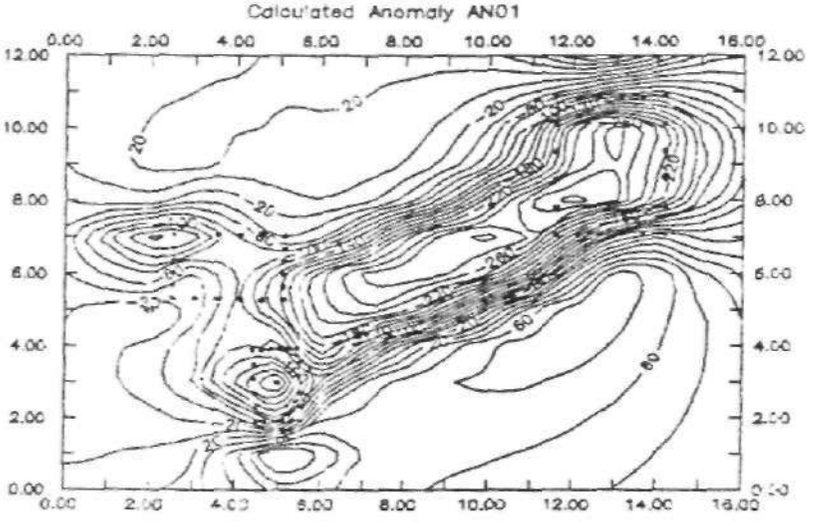


Figure 4.14(b).

× × Body outline

Table 4.11: Interpretation results of Anomaly Ano O1

body No.	a_1	a_2	b_1	b_2	h_1	h_2	Susc	Θ
	km	km	km	km	km	km	emu	degree
1	5.80	7.70	2.60	5.40	.00	5.05	0.000155	- 12.0
2	.998	3.871	6.470	14.90	.60	5.1	.00311	- 22.5
3	7.52	11.624	12.59	15.40	.53	7.6	.00502	- .500
4	1.89	4.043	4.887	6.044	.00	6.9	.00408	- 2.00

5.6.2 Anomaly number ANO2

The anomaly is located around Gana and Rurum and consist of a pair of positive and negative anomalies of nearly the same amplitude ranging from - 280 nT to 260 nT. The positive anomaly correlates with a granitic body located around the area in the geological map of the area. The anomaly has a strike direction trending roughly E-W. The shape of the anomaly is shown in Fig. 4.15a and the modeled anomaly shown in Fig 4.15b. The anomaly has been interpreted to consist of six prismatic bodies. After the 20th iteration the objective function reduced from 2,516,851.0 to 210,559.5 with a correlation of 90.7% between the observed and calculated anomaly. A constant regional of 46.97 nT has been observed in the area. The interpreted parameters of these anomaly is given in Table 4.12.

4.6.3 Anomaly number ANO 3

This anomaly is located between longitude 8.47° to 8.64° and latitude 11.75 to 11.84° east of Kura. The anomaly is a magnetic low with amplitude of -180 nT and

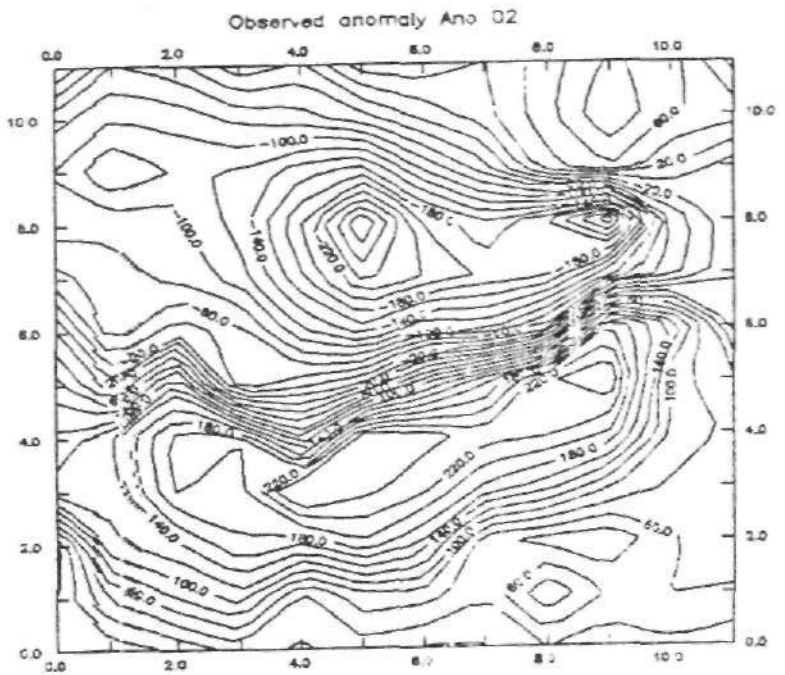


Figure 4.15(a).

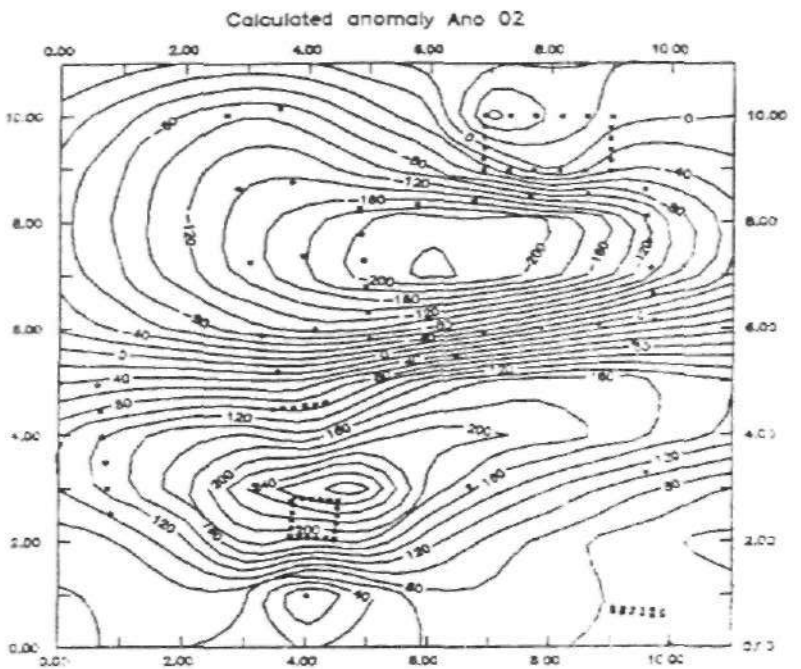


Figure 4.15(b).

× × Body outline

Table 4.12: Interpretation Results of Anomaly ANO 02

body	a_1	a_2	b_1	b_2	h_1	h_2	Susc	Θ
No	km	km	km	km	km	km	emu	degree
1.	2.635	5.259	1.124	16.966	1.215	2.409	- .00278	- 5.00
2.	2.634	3.409	3.815	4.614	.363	4.774	- .01457	5.00
3.	1.721	1.829	9.656	10.557	.00	6.587	- .00535	6.00
4.	4.281	11.829	4.354	5.304	1.89	8.40	0.1845	- 8.00
5.	5.883	8.553	5.845	10.937	.803	.811	0.00238	- 4.0
6.	9.835	10.946	7.273	9.518	.00	.137	-0.00216	1.0

uncorrelated to the granitic terrain shown in the geological map of the area but may probably due to a subsurface igneous intrusion which does not outcrop. The anomaly has a strike direction trending in the NE-SW direction. The shape of the anomaly is shown in Fig. 4.16a, and the calculated field shown in Fig. 4.16b. It is interpreted to compose of five prismatic bodies. The interpreted parameters of these bodies is given in Table 4.3. After the 20th iteration, The objective function reduced from 2,164,2973.0 to 586,440.0 and there was 91.2% correlation between observed and calculated field. A constant regional of 42.16 nT is observed in the area.

4.6.4 Anomaly number ANO 4

The anomaly is located between the longitude 8.52° to 8.60° and between latitude 11.47° to 11.52° the anomaly is centred around Rano. The anomaly is a sharp magnetic low with amplitude of -380 nT, it is uncorrelated with the granitic outcrop in the Geological map

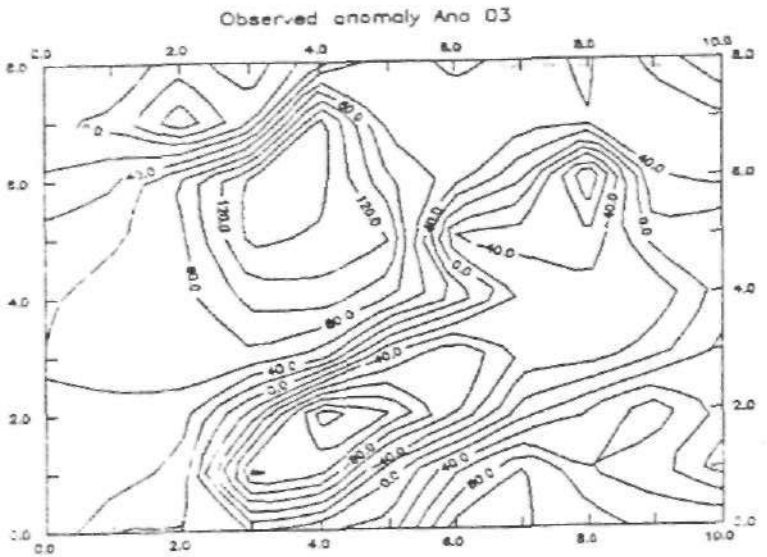


Figure 4.16(a).

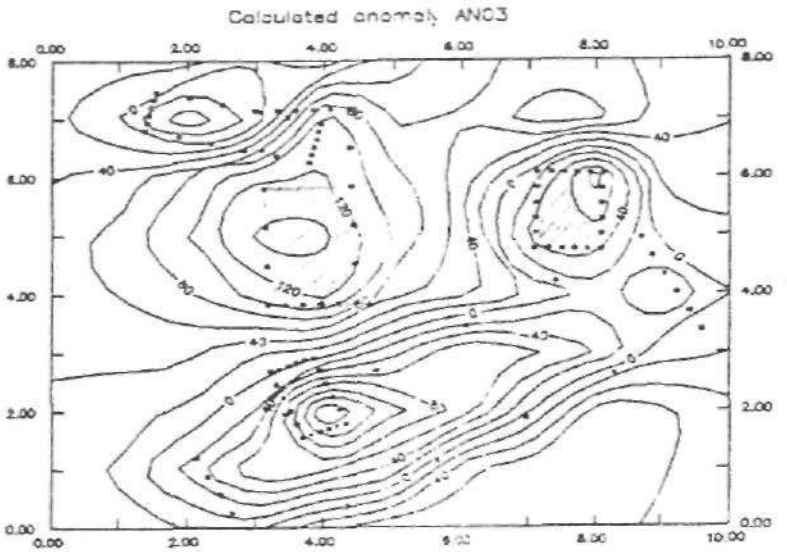


Figure 4.16(b).

× × Body outline

Table 4.13: Interpretation Results of Anomaly Ano 03

body	a_1	a_2	b_1	b_2	h_1	h_2	Susc	Θ
No	km	km	km	km	km	km	emu	degree
1.	7.516	8.253	-.193	2.475	.729	5.112	.00405	13.0
2.	4.008	7.590	3.59	4.964	0.00	4.460	-0.00203	-2.0
3.	2.645	10.816	0.016	1.980	.389	3.086	0.00143	60.20
4.	4.340	5.049	-1.349	-0.026	0.00	0.148	0.00407	67.6
5.	5.438	6.841	7.468	8.526	0.00	6.866	0.00291	2.00

but may be due to such surface igneous intrusion which does not outcrop. it has an E-W strike direction and is interpreted to be composed of four prismatic bodies. The interpreted parameters of these bodies is given in Table 4.14 while the shape of the anomaly and it modeled body is shown in Fig 4.17a and Fig 4.17b respectively. At the end of the 20th iteration the objective function reduces from 2,571,588 to 58644.0 with a correlation of 91.2% between the observed and the calculated field. A constant regional of 29.09 nT was observed in the area.

4.6.5 Anomaly number ANO 5

The anomaly is located between the longitude 8.66° to 8.80 and latitude 11.72° to 11.82°. The anomaly was not identified by the gravity survey of the Rano area conducted by Ojo *et al.*(1993). It is a magnetic low with amplitude of -420 nT, uncorrelated with the granitic terrain exposed within the geological map of the study area. It may, therefore, be

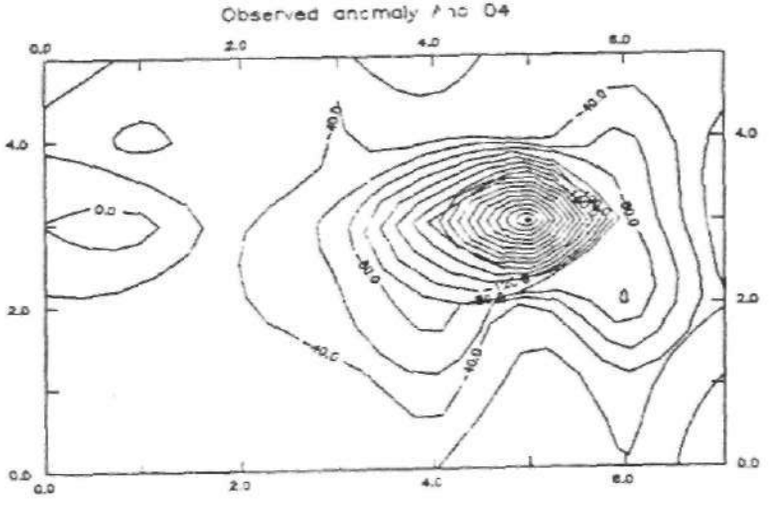


Figure 4.17 (a).

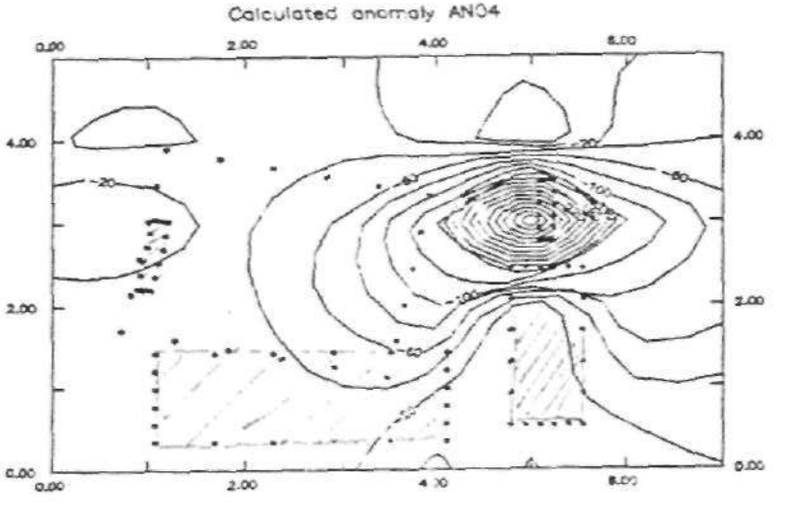


Figure 4.17 (b).

× × Body outline

Table 4.14: Interpretation Results of Anomaly Ano 04

body	a_1	a_2	b_1	b_2	h_1	h_2	Susc	Θ
No	km	km	km	km	km	km	emu	degree
1.	2.548	3.465	.610	.703	.441	4.062	-.00120	12.0
2.	1.965	4.382	3.409	6.124	.387	7.449	.00285	12.0
3.	2.996	3.782	5.495	5.664	.210	.601	.02059	0.00
4.	.587	2.628	5.178	5.996	.329	4.859	-0.00575	-3.00
5.	.373	1.536	1.165	4.441	.924	5.939		-11.00

probably due to subsurface igneous intrusion which does not outcrop. The shape of the anomaly is shown in Fig. 4.18a and the modeled anomaly in Fig. 4.18b. It is interpreted to compose of three prismatic bodies with parameters as given in Table 4.15. After the 20th iteration the objective function reduced from 908,199.8 to 208,163.1 with a 92.2% correlation between the observed and the calculated anomaly and a constant regional of -26.32 nT.

Table 4.15: Interpretation Results of Anomaly Ano 05

body	a_1	a_2	b_1	b_2	h_1	h_2	Susc	Θ
No	km	km	km	km	km	km	emu	degree
1.	4.00	7.626	-.890	14.008	1.248	8.057	0.0160	15.00
2.	4.988	6.328	3.022	9.429	.450	4.020	.00224	-4.00
3.	4.742	7.275	11.500	15.667	.204	2.708	-.00036	1.00

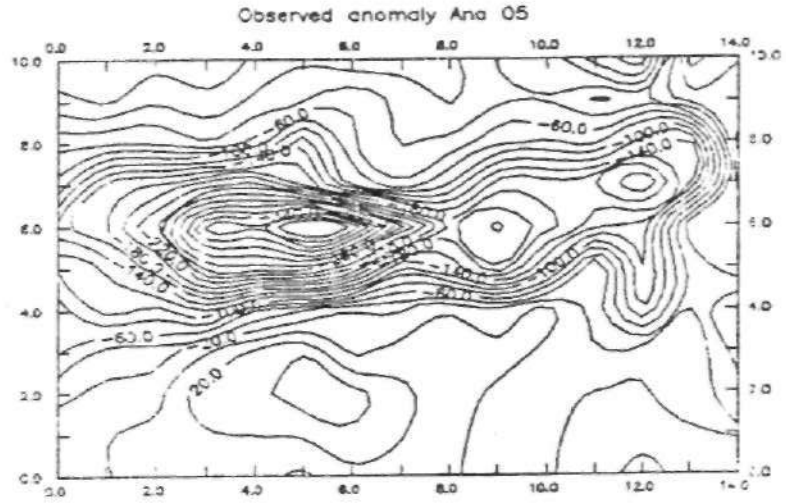


Figure 4.18(a).

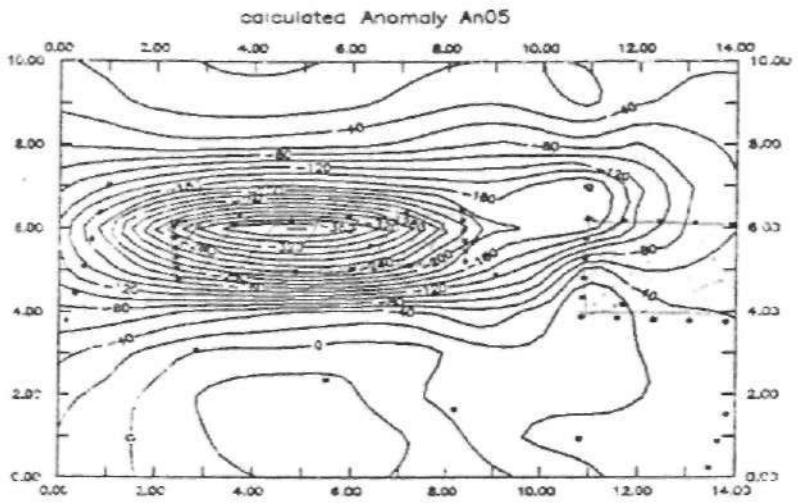


Figure 4.18(b).

× × Body outline

4.6.6 Anomaly number ANO 6

The anomaly is located between the longitude 8.90° to 9.00° and latitude 11.53° to 11.61°. Like the anomaly ANO 5, this anomaly was not identified by the Gravity survey (Ojo *et, al* 1993). It is uncorrelated with any surface rock in the geological map of the area but may be due to subsurface igneous intrusion which does not outcrop and has an amplitude of -360 nT, and an E-W strike direction. The shape of the anomaly is shown in Fig. 4.19a and the modeled anomaly shown in Fig 4.19b. It is interpreted with five prismatic bodies. The interpreted with parameters as given in Table 4.16 and a correlation of 89.9% is observed between the calculated and the observed anomaly. A constant regional of 61.41 nT is found in the study area. The interpretation suggest that the anomaly is made up of basic igneous rock intruded on an acidic granite.

Table 4.16: Interpretation Results of Anomaly ANO 06

body	a_1	a_2	b_1	b_2	h_1	h_2	Susc	Θ
No	km	km	km	km	km	km	emu	degree
1.	3.134	6.466	.110	5.688	.572	4.216	.00267	11.00
2.	4.093	4.520	.768	2.001	.032	.482	.00401	-7.00
3.	4.247	5.622	4.639	5.256	.245	.280	.0833	.000
4.	1.754	2.664	1.502	4.237	.882	8.628	- .00231	4.000
5.	6.771	7.339	2.023	3.240	00.00	2.435	.00614	2.00

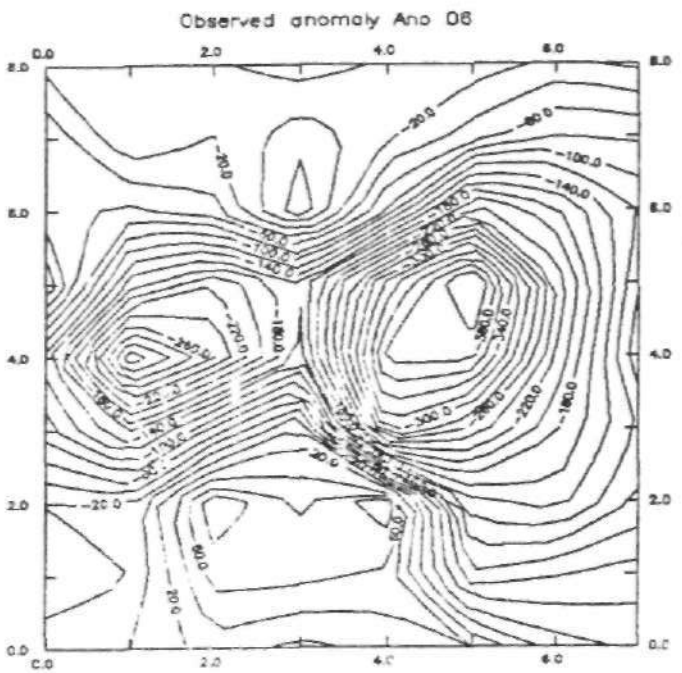


Figure 4.19 (a).

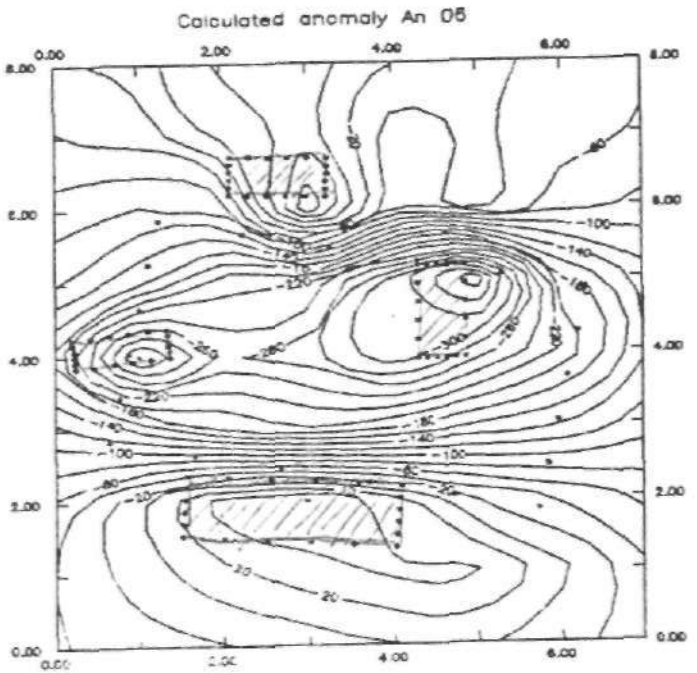


Figure 4.19 (b).

× × × × × × Body outline

4.6.7 Anomaly number ANO 7

The anomaly is part of the anomaly (ANO 3) which is centred around Kumarya and Karfi. This anomaly could be isolated as an independent from the body of the anomaly. It is located between the longitude 8.55° to 8.60° and latitude 11.72° to 11.77°. It is a magnetic low with amplitude of - 160 nT. It has a NE-SW strike direction and uncorrelated to the surface geology of the area. It may be probably due to subsurface igneous intrusion which does not outcrop. The shape of the anomaly is shown in Fig. 4.20a and the modeled anomaly is shown in Fig 4.20b. It is interpreted to compose of four prismatic bodies, with parameters as given in Table 4.6.7 with a 90.8% correlation between the observed and the calculated field and a constant regional of 23.96 nT observed in the study area.

Table 4.17: Interpretation Results of Anomaly Ano 07

body	a_1	a_2	b_1	b_2	h_1	h_2	Susc	Θ
No	km	km	km	km	km	km	emu	degrees
1.	1.503	3.210	-3.124	-.939	0.00	2.125	.00299	87.00
2.	4.560	4.860	-0.039	1.259	0.00	3.11	.00348	45.00
3.	1.240	2.248	-2.146	0.390	0.00	8.070	-0.00264	73.00
4.	2.941	3.073	3.142	8.939	0.00	4.574	-0.01575	1.00

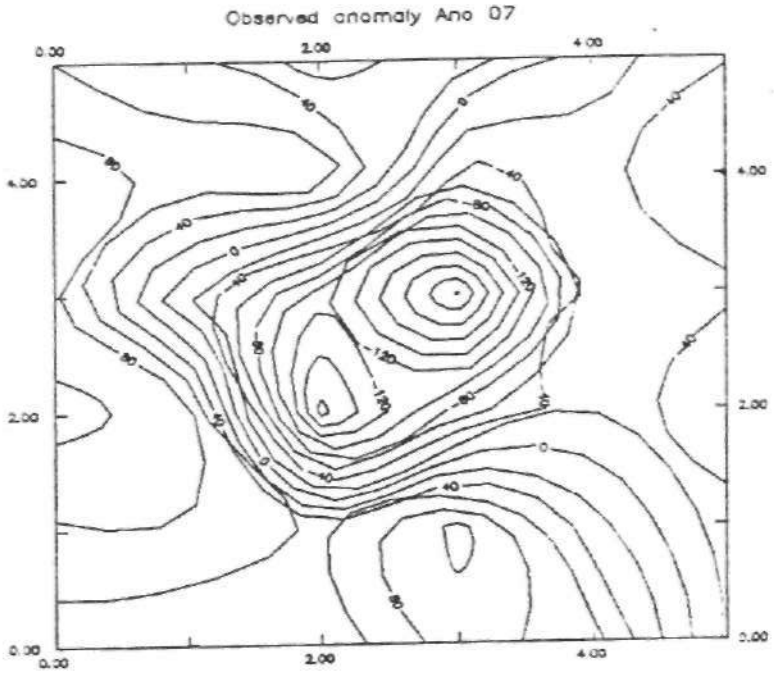


Figure 4.20(a).

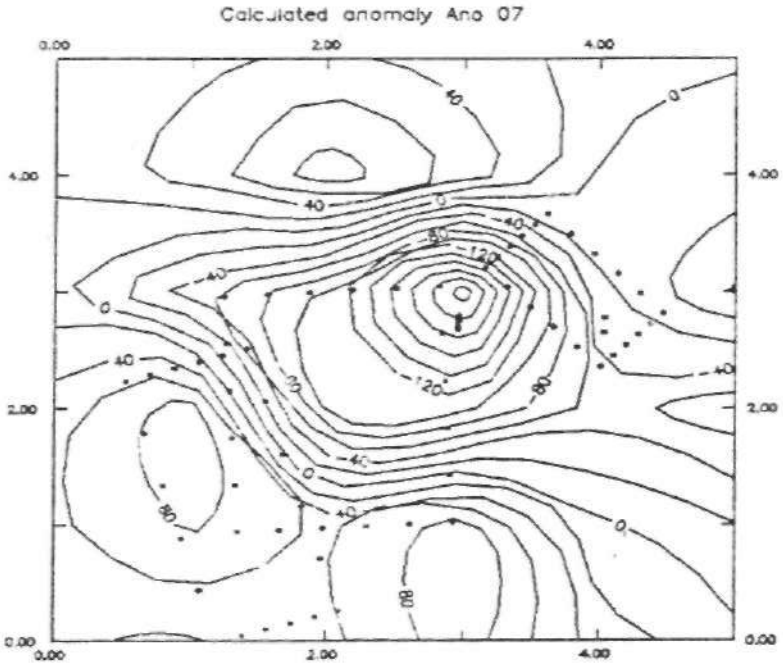


Figure 4.20(b).

× × Body outline

CHAPTER FIVE

CONCLUSIONS AND RECOMMENDATIONS

5.1 CONCLUSIONS

The interpretation of the aeromagnetic data for the area occupying part of the Precambrian basement of Kano State reflect important features which show the structural trend of the area. The regional and upward continuation map of the study area reflect deeper magnetic anomalies of regional scale and have E-W trend, which may have an important role in the emplacement of mineralized bodies within the study area. The residual map and the second vertical derivative map clearly reflect shallow and near surface highly magnetized bodies which correlate well with the previous gravity survey of the area by Ojo *et al.* (1993).

A residual magnetic low of amplitude of about -32 nT, 8km south west of Dal correlates with the residual gravity high of amplitude -42 mGal and poorly exposed basic igneous intrusion in the geological map of the area. Other magnetic lows which did not correlate well with the surface geology are believed to be due to basic intrusions which do not outcrop. The positive magnetic amplitude anomalies are interpreted to be due to acidic igneous intrusions and correlate with the granite bodies of the study area.

Most of the residual anomalies are oriented in the NE-SW direction (Fig 4.4) Although there are no mine locations within the study area this orientation suggests the presence of shear zones with magnetic mineralization, especially with the basic igneous intrusions which are believed to be associated with ore mineral such as illiminite and magnetite. The second vertical derivative map also reveal various contacts between rock

units with contrasting susceptibility. This correlates with the geological boundries identified in the geological map of the area.

The lineament studies of the area which include the orientational and non-orientational analyses, the regional-residual separation, the upward continuation, auto correlation and second vertical derivative shows the area to be characterized by NE-SW trending, residual anomalies super imposed on an E-W regional field. The correlation of the E-W regional with the result earlier obtained by Ajakaiye (1979) and Amusu (1986) suggest their wider extent and this shows that they are the structures exploited during the emplacement of the granite masses in the study area. This also confirm the belief by some geologist that the Pan-African Orogeny which emplaced the granite masses have exploited the existing structures and altered the structure of the basement, giving it its present shape. The relics structures are still preserved within the basement as an E-W trend (Section 4. 4).

The 3-Dimensional modeling of some of the selected residual anomalies shows that the basic igneous rocks have depths to the Top ranging from 0.00 km to 1.74 km and the depth to the bottom from 0.60 km to 8.638 km; while the acidic rocks have much shallower depth extent with depth to the top from 0.00 km to 0.400 km and depth to the bottom from 0.200 km to 5.26 km. These correlates with earlier results obtained by Ojo *et al.* (1993) who showed that the basic igneous rocks are buried at much deeper depth than the granite bodies.

Some of the modeled anomalies have very small depth extent and occur as sill. This suggests evidence of lava flow which spread on top of other granite masses. Another alternative suggestion to the occurrence of this thin bodies is that it may be due to

weathering process which have weathered the bodies and erosion have carried away part of the weathered rocks. Some geologist have argued that the older granites are as a result of magmatic emplacement or through metasomatism whereby sediment and metamorphic rocks were converted to granites by metasomatic migration of materials.

Although the problems of the origin of the older granites cannot be resolved from the interpreted models because of the reason of the limited area of study, the interpreted models suggest that the granites are not very deep in extent. These findings contrasted with the results obtained in the studies by Gandu etal. (1986), Udensi *et al.* (1986), Adeniyi (1987) and Osazuwa *et al.* (1992) in Malumfashi, Minna and Zaria areas respectively. They all showed that the granites where relatively deep in extent. The result of this study therefore tends to agree with the suggestion that metasomatism must have reached an advanced stage, in the area (G.S.N, Unpublished Geological report), and therefore suggested that the older granites of Nigeria may vary in their origin.

5.2 RECOMMENDATION

To fully resolve the problem of origin of the granite masses in the Nigeria basement complex, it is recommended that a detailed integrated geophysical and geochronological studies be carried out in the whole of the Nigerian Basement Complex. In addition, a detailed ground magnetic follow-up survey should also be made in the areas identified as basic igneous rocks in order to assess their economic minerals potentials. This work also shows the need to carry out a detailed structural map of the Nigerian Basement Complex in conjunction with other geophysical data.

REFERENCES

1. Agarwal,R.G. and Kanasewich,E.R (1971)Automatic trend analysis and interpretation of potential field data . Geophysics, 36(2):339-648

2. Adeniyi, O.O (1987) Gravity Survey of the older granite Plutons in Zaria area of Kaduna State, Nigeria. Unpublished M.Sc Thesis, Ahmadu Bello University, Zaria.

3. Ajakaiye, D.E, (1975) A Gravity Survey over the Nigerian Younger Granite Province in C.A Kogbe (Ed) Geology of Nigeria. Elizabethan publishing Co.

4. Ajakaiye, D.E and Verheinjen P.J.T (1979) Gravity Survey across the Quartenary Basement Areas of Kano State. Jour of mining and Geol. Nigerian, (14) 55. Abstract.

5. Alli, S. (1989) Analysis of Aeromagnetic Data from two Schist Belts in NW Nigeria. Unpublished M.Sc. Thesis Ahmadu Bello University, Zaria.

6. Am, k. (972) The Arbitrary Magnetized dyke, Interpretation by Characteristics curves Geo Exploration 10, 63-90.

7. Amosu, S.N. (1982) A Gravity Survey of the Dutse Younger granite Complex, Kano State, Nigeria. Unpublished M.Sc. Thesis Ahmadu Bello University Zaria.

8. Bath, M. (1974) Spectral Analysis in Geophysics Elsevier pub. Co., Amsterdam.

9. Bhattacharyya, B.K. (1964) Magnetic Anomalies due to prism shaped bodies with arbitrary polarization; Geophysics (29), 517-531.

10. Bhattacharyya, B.K. and Lue, L.K. (1975) Analysis of magnetic Anomalies over yellow stone National park: Mapping of curie point isothermal surface for Geothermal reconnaissance Journal of Geophysical research 80(32) 4461-4465.

11. Bhattacharyya, B.K. (1972), A generalized Multi body Model for Inversion of Magnetic Anomalies Geophysics (45) 255-270.

12. Bott M.H.P (1953) A Geophysical study of the granite problem. Quart of J. Geol. Soc. London Vol. 1, No. 112, 1145-69.

13. Branov W. (1975) Potential Fields and Their Transformations in Applied Geophysics. Geo Explorations Monographs Series Geopublication Associates. Berlin Stuttgart.

14. Coles, R.L (1976), A flexible iterative magnetic anomaly Interpretation Technique using Multiple Rectangular prisms, Geo exploration (14) 125-141.

15. Dambatta, U.A. (1990) Outline Geology of Kano State. Departmental Seminar series, Department of Geology Ahmadu Bello University Zaria. p 43.

16. Dobrin , M.B., (1982) Introduction to Geophysical prospecting McGrain Hill, London.

17. Falconer, J.D. (1911) The Geology and Geography of Northern Nigeria, London, Macmillan and Company.

18. Gandu, A.H., Ojo, S.B; and Ajakaiye, D.E. (1986) A Gravity Study of the Precambrian Rocks in the Malumfashi Area of Kaduna State, Nigeria. Tectonophysics, 126 pp 181-194.

19. Gay, P.S. Jr. (1972) Fundamental Characteristics of Aeromagnetic Lineaments, their geological significance and their significance to Geology. Streo mapco. Utah. 90P.

20. Gay, P.S. Jr., (1967) Curves for Interpretation of magnetic anomalies caused by two dimensional structures. In Mining Geophysics 11, SEG., Tulsa OK., 512-548.

21. Gerard, A and Debglia N. (1975) An Automatic Three-Dimensional Modelling for Interpretation of Gravity or Magnetic Anomalies, Geophysics (40) 1014 - 1034.

22. Ghazala, H.H. (1993) Geological and Structural Interpretation of Airborne Surveys and its Significance for Mineralization, South Eastern Desert, Egypt. Jour of African Earth Science Vol.16 (3) pp 273 - 283.

23. Grant, N.K. (1969) The Late Precambrian to early Paleozoic Pan-African Oregency in Ghana, Togo, Dahomey and Nigeria. Geol. Soc. of Am. Bull Vol. 80 pp 45 - 46.

24. Hahn, A., Kind, E.G and Mishra, Dic (1976), Depth estimation of magnetic source by means of Furrier Amplitude spectra. Geop Pros. 24, pp 278 - 308.

25. Hall, D.H. (1968) A Magnetic Interpretation Method for Calculating body Parameters for buried sloping steps and thick sheets. Geoexploration 6, 187 - 206.

26. Hjelt, S.E. (1973), Experience with Automatic Magnetic Interpretation using the thick plate Model. Geophysical Prospecting 21, 243 - 265

27. Horton, C.W ; W.B. Hempkins, and A.A.J Hoffman; (1964) A statistical Analysis of Aeromagnetic maps from the North-western Canadian shield. Geophysics vol xxix, No.4, pp 582 - 601.

28. Johnson, W.W. (1969) A Least Square Method of Interpreting Magnetic Anomalies Caused by Two-Dimensional Structures. Geophysics, 34, 65 - 74.

29. Kangkolo,R. (1996) A detailed magnetic interpretation of the Mfe basin Unpublished P.hd thesis Ahmadu Bello University Zaria.

30. Koulomzine, T.Y., Lamontage and A. Naoleau, (1971) New Method for Direct Interpretation of Magnetic Anomalies caused by Inclined Dykes of Infinite Length. Geophysics (35) 812 - 830.

31. Kunaratnam, K. (1981) Simplified Expression for Magnetic Anomalies due to Vertical Rectangular Prisms. Geophy - prosp., (29) 883 - 890.

32. McCurry, P. (1971). The Geology of the Precambrian to Lower Paleozoic Rocks of Northern Nigeria, a review in C.A Kogbe (Ed) Geology of Nigeria, Elizabethan Publishing Co. Lagos, 30.

33. McCurry, P. and Wright, J.B (1971), On Place and Time In Orogenic Granite Plutonism, Geol Soc of Am Bull, Vol 82, pp 1413 - 1476.

34. Mc Curry, P. and Wright, J.B. (1970) Geochemistry of Calc-alkaline Volcanics In North-Western Nigeria and a possible Pan African Suture Zone. Earth Planet Sci letts V.37. p 90 - 96.

35. McCurry, P. (1975). The Geology of the Precambrian to Lower Paleozoic Rocks of Northern Nigeria, a review in C.A Kogbe (Ed) Geology of Nigeria Elizabethan Publishing Co. Lagos p 15 - 39.

36. McCurry ,P., (1970). The geology of degree sheet 21 (Zaria). Unpublished M.sc. Thesis, Ahmadu Bello University, Zaria.

37. McGrath, P.H and P.J. Hood (1973) An Automatic Least Square Multi Model Method for Magnetic Interpretation Geophysics, 38, 349 - 358.

38. McGrath, P.H. and P.J. Hood (1970) The Dipping Dyke Case a Computer Matching Method of Magnetic Interpretation Geophysics (35) 831 - 848.

39. Naidu, P.S. (1969) Estimation of Spectrum and Cross Spectrum of Aeromagnetic Field Using Fast digital F rrier Transform ((FDET) Techniques. Geophy. Prosp. XVII pp 344 - 361.

40 Naidu, P.S. (1970a) Statistical Structure of Aeromagnetic Field. Geophysics 35(2) pp 279 - 292.

41. Naidu, P.S. (1970b) Furrier Transform of Large Scale Aeromagnetic Field Using Modified Version of FFT. pageoph 81(4); pp 17 - 25.

42. Mullan, H.S. (1979) Structural Distinction Between a Meta Sedimentary Cover and an Underlying Basement in the 600 my old Pan-African Domain of North Western Nigeria Discussion. Geol. Soc Amer Bull. V. 90 pp 983 - 984.

43. Ogezi, A.E. (1977), Geochemistry and Geo Chronology of Basement Rocks of NW Nigeria, Unpublished Ph.D Thesis Univ. Leeds 295 pp.

44. Ojo, S.B, Osazuwa, I.B. and Oladosu M.O. (1993), A Gravity Survey of the Igneous Intrusions in the Rano Area of Kano State. Intern. Jour. of BioChemiphysics, Vol. 2, Nos. 1 & 2, pp 130 - 136.

45. Oladusu, M.O. (1987) A Gravity Survey of the Igneous Intrusions in the Rano Area of Kano State, Nigeria Unpublished M.Sc. Thesis Ahmadu Bello University Zaria.

46. Oluyide, P.O. (1988), Structural Trends In the Nigeria Basement Complex, A Review in the Precambrian Geology of Nigeria. Published by the Geological Survey of Nigeria pp 93 - 97.

47. Osazuwa, I.B, Adeniyi, O.O and Ojo, S.B (1992) A gravity study of the older granite suite in the Zaria Area of Kaduna state, Nigeria. Journal of Mining and Geology, Vol. 28, No. 2, pp 231-236.

48. Oyawoye, M. O (1964) The Geology of the Nigerian Basement Complex. Journ of Mining and Geol Nigeria 1, 87 - 102.

49. Rahaman, M.A (1978), Review of the Basement Geology of South Western Nigeria In; Kogbe, C.A (Ed), Geology of Nigeria, Lagos, Nigeria. Elizabethan Publishing Co., 41 - 58.

50. Rahman, M.A and Ocan, O.O. (1978) On Relationships In the Precambrian Migmatite Gneisses of Nigeria. Journ. Mining and Geol., Vol. 15, No. 1, p 23 - 32.

51. Rahaman, M.A. (1988) Recent Advances in the Study of the Basement Complex of Nigeria. In the Precambrian Geology of Nigeria. A Publication of the Geological Survey of Nigeria.

52. Rao, D.B. and N. Ramesh Babu (1991) A Rapid Method for Three-Dimensional Modelling of Magnetic Anomalies Geophysics 58, (11) pp 1729 - 1737.

53. Rao, B.S.R, I.V.R Murthy and C.V. Rao; (1973) Two Methods for Computer Interpretation of Magnetic Anomalies by Dykes. Geophysics (38) 710 - 718.

54. Henderson, R.G and Isidore Zietz; (1960) The computation of Second Vertical Derivatives of Geomagnetic Field. Geophysics (14) pp 107.

55. Russ, W. (1957) The Geology of Pasts of Niger, Zaria and Sokoto Provinces with Special Reference to the occurrences of Gold. Bull. Geol Surv. Nigeria No. 27.

56. Truswell, J.F and Cope, R.N. (1963) The Geology of Parts of Niger and Zaria Provinces Northern Nigeria Bull Geol. Surv. Nigeria. No. 29. 52 pp.

57. Turner, D.C. (1983) Upper Proterozoic Schist Belts in the Nigerian Sector of the Pan African Province of West Africa. Precambrian Research, 21 55 - 79

58. Udensi, E.E, Ojo, S.B. and Ajakaiye D.E. (1986) A Three-Dimensional Interpretation of Bouguer Anomalies over the Minna Batholith in Central Nigeria. Precambrian Research, 32, 1 - 5.

59. Gupta, V.K. and Ramani, N. (1982) Optimum second vertical derivatives in geologic mapping and mineral exploration. Geophysics, Vol. 47, 12. p 1706 - 1715.

60. Whitehill D. E, (1973) Automated Interpretation of Magnetic Anomalies Using the Vertical Prism Model Geophysics, (38) 1070 - 1087.

61. Won, I.T. (1981) Application of Gauss's Method to Interpretation of Magnetic Anomalies of Dipping Dykes Geophysics (46), 211 - 215.